The reaction kinetics and film morphology of molybenum films deposited by LPCVD on a silicone surface

by Edward James Flanigan

A thesis submitted in partial fulfillment of the requirements for the degree of Master of Science in Chemical Engineering

Montana State University

© Copyright by Edward James Flanigan (1987)

Abstract:

Molybdenum films were deposited by Low Pressure Chemical Vapor Deposition (LPCVD) on silicon substrates by the hydrogen reduction of molybdenum hexafluoride. The reaction kinetics were studied in order to determine a rate equation. Extensive scanning electron microscopy (SEM), electron spectroscopy for chemical analysis (ESCA), auger electron spectroscopy (AES) and rutherford back-scattering (RBS) studies were conducted to characterize and analyze the morphology of the deposited molybdenum films.

The hydrogen reduction of molybdenum hexafluoride was determined to be one half order in hydrogen, approximately zero order in molybdenum hexafluoride and had an activation energy of 76,000 J/mol at temperatures from 250 to 3507deg;C, and total pressures from 0.9 to 10.0 torr. The preexponential factor was determined to be 2.02 x 106 nm s-1.torr -0.5.

The main features of the films were the high oxygen (up to 28%) and impurity content. Although pores could not be seen by the instrumental techniques provided, film impurities and surface roughness were attributed to a porous deposit. Rough interface conditions were explained by the competing silicon reduction reaction, and good quality deposits were seen to be produced at high temperatures and low pressures.

Results of this experiment were compared with previous studies involving tungsten and molybdenum LPCVD. One difference observed was the apparent lack of linear film growth with time. The other difference was that a molybdenum film had a resistivity of three times less than any previously reported resistivity for a LPCVD molybdenum film.

THE REACTION KINETICS AND FILM MORPHOLOGY OF MOLYBDENUM FILMS DEPOSITED BY LPCVD ON A SILICON SURFACE

by

Edward James Flanigan

A thesis submitted in partial fulfillment
of the requirements for the degree

of

Master of Science

in

Chemical Engineering

MONTANA STATE UNIVERSITY

Bozeman, Montana

July 1987

MAIN LIB.
N378
F6145
Cop. 1

APPROVAL

of a thesis submitted by

Edward James Flanigan

This thesis has been read by each member of the thesis committee and has been found to be satisfactory regarding content, English usage, format, citations, bibliographic style, and consistency, and is ready for submission to the College of Graduate Studies.

Sept. 2, 1987
Date

Chairperson, Graduate Committee

Approved for the Major Department

July 7, 1987
Date

John T. Sears
Head, Major Department

Approved for the College of Graduate Studies

September 2, 1987
Date

Henry L Parsons
Graduate Dean

STATEMENT OF PERMISSION TO USE

In presenting this thesis in partial fulfillment of the requirements for a Master's degree at Montana State University, I agree that the Library shall make it available to borrowers under rules of the Library. Brief quotations from this thesis are allowable without special permission, provided that accurate acknowledgment of source is made.

Permission for extensive quotation from or reproduction of this thesis may be granted by my major professor, or in his/her absence, by the Director of Libraries when, in the opinion of either, the proposed use of the material is for scholarly purposes. Any copying or use of the material in this thesis for financial gain shall not be allowed without my written permission.

Signature Edward J. Flanigan

Date 7/10/87

TABLE OF CONTENTS

	Page
TITLE PAGE	i
APPROVAL	ii
STATEMENT OF PERMISSION TO USE	iii
TABLE OF CONTENTS	iv
LIST OF TABLES	vi
LIST OF FIGURES	vii
ABSTRACT	ix
INTRODUCTION	1
BACKGROUND	5
Integrated Circuit Technology	5
Importance of Molybdenum as a Contact or Interconnect Metal	5
Molybdenum Deposition (Basic Reaction)	9
Hydrogen and Silicon Reduction of Molybdenum Pentachloride	10
Hydrogen and Silicon Reduction of Tungsten Hexafluoride	13
Hydrogen Reduction of Molybdenum Hexafluoride	14
Analyses by AES	16
Analyses by SEM	18
Analyses by ESCA	20
Analyses by RBS	22

RESEARCH OBJECTIVES 24

EXPERIMENTAL EQUIPMENT 25

Gas Flow Control System 25
Reactor and Heater 27
Pressure Read-Out and Control System 29
Pumping System 29
Acid Gas Detection System 30
After Burner and Alumina Trap System 31
Chemical Hazards 32

EXPERIMENTAL PROCEDURES 34

Sample Cleaning 34
Deposition Procedure 34
AES Analysis Procedure 35
SEM Analysis Procedure 38
ESCA Analysis Procedure 38
Acid Dissolution Procedure 39
RBS Analysis Procedure 39

RESULTS AND DISCUSSION 40

Thickness Determination of Deposited Samples . . . 40
Reaction Kinetics 40
Order of Reaction 43
Rate Equation 46
Characterization of Molybdenum Films 48

SUMMARY AND CONCLUSIONS 70

RECOMMENDATIONS 72

REFERENCES CITED 73

APPENDICES 78

Appendix - Sample Calculations 79

LIST OF TABLES

Table		Page
1.	Free Energy Changes for the MoF_6 Reaction . . .	10
2.	Temperature, Time and Partial Pressure Variations for the Kinetic Study of the Hydrogen Reduction of Molybdenum Hexafluoride .	36
3.	Molybdenum Film Thickness Measurements by Acid Dissolution (for the Kinetic Data)	41
4.	Relative Molybdenum Film Impurities from AES Depth Profiles at Molybdenum's Highest Peak Value	50

LIST OF FIGURES

Figure		Page
1.	Schematic View of a MOSFET Cross Section	6
2.	LPCVD Reactor System	26
3.	Substrate Heater/Holder for the LPCVD Reactor .	28
4.	Molybdenum Thickness as a Function of Time at T = 300 °C and P_{tot} = 0.9 torr	42
5.	Arrhenius Plot	44
6.	Plot for Determining Order of Reaction With Respect to Hydrogen Partial Pressure	45
7.	Plot for Determining Order of Reaction With Respect to Molybdenum Hexafluoride Partial Pressure	47
8.	AES Depth Profile of a Mo Film Deposited at T = 300 °C and P_{tot} = 4 torr	49
9.	ESCA Spectra for a Mo Film Deposited at T = 350 °C and P_{tot} = 5 torr	52
10.	SEM Surface Micrograph of a Mo Film Deposited at T = 400 °C and P_{tot} = 0.9 torr	55
11.	SEM Surface Micrograph of a Mo Film Deposited at T = 250 °C and P_{tot} = 2.5 torr	56
12.	SEM Surface Micrograph of a Mo Film Deposited at T = 300 °C and P_{tot} = 1.3 torr	58
13.	SEM Surface Micrograph of a Mo Film Deposited at T = 250 °C and P_{tot} = 7.3 torr	59
14.	SEM Surface Micrograph of a Mo Film Deposited at T = 350 °C and P_{tot} = 5 torr	61
15.	AES Elemental Point Scan of the Surface in Figure 14(b); point 1	62

Figure | Page

16. AES Point Elemental Scan of the Surface in Figure 14(b); point 4 63

17. Rutherford Backscattering Scan of Mo Films . . . 65

18. SEM Cross-Section of a Mo Film Deposited at $T = 350\ ^{o}C$ and $P_{tot} = 5$ torr 67

19. SEM Cross-Sections of a Mo Film Deposited at $T = 400\ ^{o}C$ and $P_{tot} = 0.9$ torr 68

ABSTRACT

Molybdenum films were deposited by Low Pressure Chemical Vapor Deposition (LPCVD) on silicon substrates by the hydrogen reduction of molybdenum hexafluoride. The reaction kinetics were studied in order to determine a rate equation. Extensive scanning electron microscopy (SEM), electron spectroscopy for chemical analysis (ESCA), auger electron spectroscopy (AES) and rutherford back-scattering (RBS) studies were conducted to characterize and analyze the morphology of the deposited molybdenum films.

The hydrogen reduction of molybdenum hexafluoride was determined to be one half order in hydrogen, approximately zero order in molybdenum hexafluoride and had an activation energy of 76,000 J/mol at temperatures from 250 to 350°C, and total pressures from 0.9 to 10.0 torr. The preexponential factor was determined to be 2.02×10^{6} nm$\cdot$s$^{-1}\cdot$torr$^{-0.5}$.

The main features of the films were the high oxygen (up to 28%) and impurity content. Although pores could not be seen by the instrumental techniques provided, film impurities and surface roughness were attributed to a porous deposit. Rough interface conditions were explained by the competing silicon reduction reaction, and good quality deposits were seen to be produced at high temperatures and low pressures.

Results of this experiment were compared with previous studies involving tungsten and molybdenum LPCVD. One difference observed was the apparent lack of linear film growth with time. The other difference was that a molybdenum film had a resistivity of three times less than any previously reported resistivity for a LPCVD molybdenum film.

INTRODUCTION

In the semiconductor industry today, aluminum is a well known and important metal. This metal is used for contacts and interconnects in the microelectronics area of very large scale integration (VLSI). Competition in the semiconductor industry is growing at a rapid pace, though. This competitive condition brings about the need for a new metal with the capabilities of making smaller, less expensive and more productive components for integrated circuits.

Aluminum is the most widely used material for metallization of silicon devices due to its low room temperature resistivity and excellent adhesion to SiO_2 and other deposited silicate glasses [1]. However, aluminum has a relatively low melting point ($660^{o}C$), and upon approaching this temperature the transfer of momentum from electrons is increased, causing transport, or migration, of the conductive material. This electromigration is a potential source of breakdown in aluminum interconnect lines [2,3].

The failures brought about by using aluminum has opened the door to new contact metals such as the refractory metals of molybdenum, tungsten and tantalum. Recently, molybdenum has shown potential applications not only as a contact or interconnect, but in other areas as well. Molybdenum silicides have been formed on refractory metals to protect Schottky diodes have been shown to approximate the ideal the

metal against high temperature oxidation [4-6]. Mo/Si characteristic properties of Schottky diodes [7]. Molybdenum has been used for diffusion or corrosion barriers and, because of its high ductility, for parts with complex shape [8]. There has also been considerable interest in molybdenum as a gate electrode for VLSI fabrication [9,10].

Molybdenum as a contact metal has shown promise in VLSI because of its high melting temperature (2610 ^{o}C), high corrosion resistance, low resistivity and expansion coefficient that is close to that of silicon. A low interconnect resistance and thus a high operating speed can also be obtained by using molybdenum [10].

Today, modern surface science and other techniques provide the capability of studying metal films designed for use in microelectronics. These methods allow the researcher to investigate such things as the uniformity and purity throughout film deposits, the porosity of a deposited film, and the condition of the interface after a metal is deposited on a surface. This film morphology is greatly affected by the deposition parameters and the rate of deposition. In chemical vapor deposition (CVD), the main parameters of the reaction are the substrate temperature, the pressure of the reactant gas mixture and the ratio of

hydrogen to metal halide. The separate variation of these parameters has great influence on the deposition rate, on the amount of impurities, on the crystal structure and grain size, and on the number of micro-bubbles that may develop under certain circumstances along the grain boundary during the reaction [11]. Improved knowledge of the film morphology and the kinetics of the reaction may provide a more efficient metal contact and manufacturing process for the semiconductor industry.

Research on the low pressure chemical vapor deposition (LPCVD) of molybdenum is limited. Several studies used molybdenum pentachloride as the source of molybdenum [7,9,12-16]. Some studies have used the carbonyl as the source of Mo [17-20]. Schottky barriers or diodes were formed by selective deposition of molybdenum [7,21] and Mo layers have been formed on n-type polysilicon lines [22]. Other authors have studied the silicides formed by molybdenum deposition [23,24] or have studied molybdenum deposits for metallurgical applications which require high deposition rates, high temperatures and atmospheric pressures in order to cover a large area. A few authors have considered the hydrogen reduction of molybdenum hexafluoride for integrated circuit technology [25,26].

In this study, molybdenum was deposited on a silicon surface by hydrogen reduction of molybdenum hexafluoride.

This was performed over a temperature range of 250-350°C and a total pressure range of 0.9-10.0 torr. The objective of this research was to investigate the molybdenum film morphology and study the kinetics of the molybdenum deposition. The amount of deposition was determined by acid dissolution of the molybdenum films. This acid dissolution method was employed in determining a reaction rate equation. The film morphology was studied by Scanning Electron Microscopy (SEM), Auger Electron Spectroscopy (AES), Electron Spectroscopy for Chemical Analysis (ESCA) and Rutherford Backscattering (RBS).

BACKGROUND

Integrated Circuit Technology

Electronics basically began with the integrated circuit (IC) which was invented by Kilby in 1958 [2]. From the early primitive forms, IC's have evolved into complex electronic devices containing hundreds of thousands of individual components on a single chip of silicon.

The transistor is the most important component of an IC. This is what tells current to flow or not, or a circuit to open or close. One such type of transistor is the metal oxide field effect transistor (MOSFET) pictured in Figure 1. This has an n-type source and drain implanted in a p-type substrate. The letters n and p refer to negative and positive charge carriers, respectively. The source and drain are contacted by metal (e.g. Al or Mo) contacts and connected to a power supply. When a threshold voltage (V_T) is applied to the gate electrode, current flows between the source and drain. This voltage creates a field across the gate oxide which causes the adjacent p substrate to invert to n-type, thus creating a conductive n channel between the source and drain [2].

Importance of Molybdenum as a Contact or Interconnect Metal

Metallization, as described above, has many important

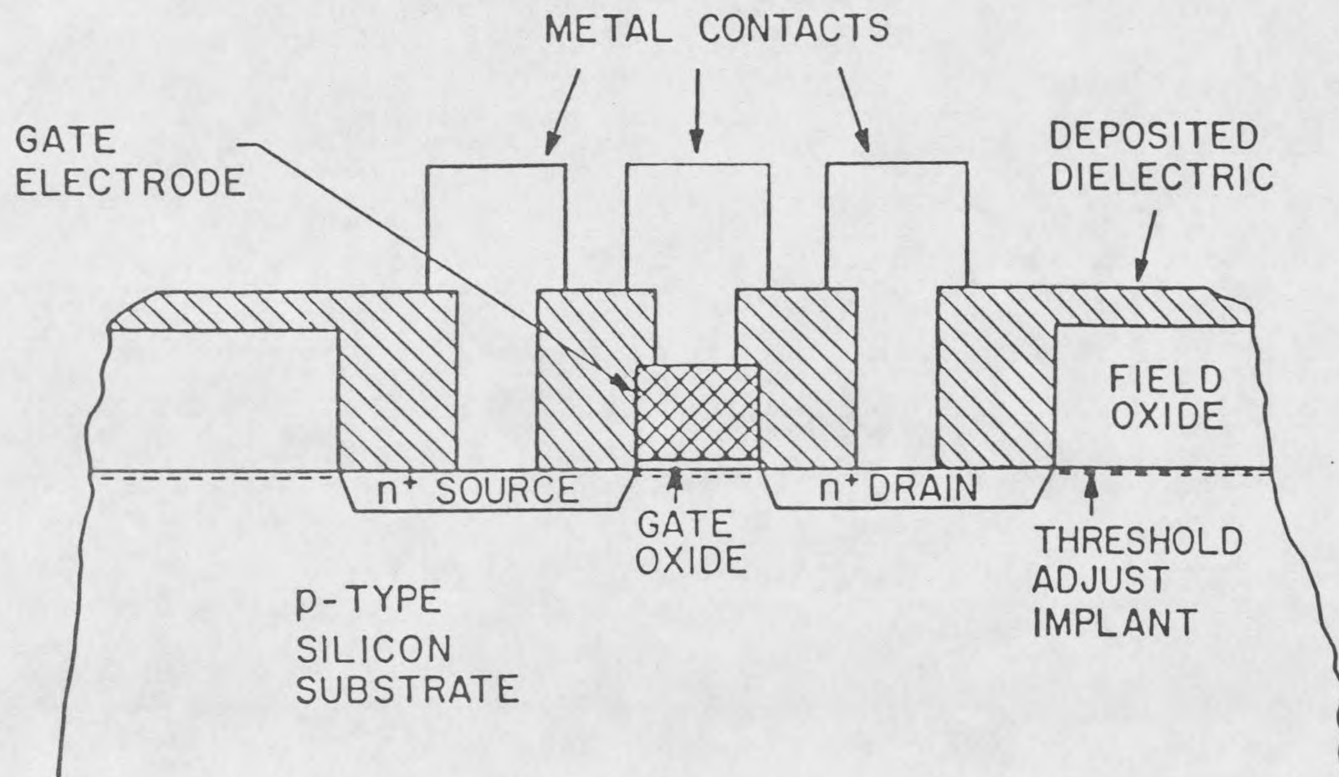

Figure 1. Schematic View of a MOSFET Cross Section

factors associated with the type of contact or interconnect used. Metallization requires a contact to have good mechanical properties, adhere firmly during both formation and subsequent processing, not cause excessive stress in the underlying semiconductor and have low electric resistance. A contact must also be compatible with the metal system used for the interconnection technology, not be susceptible to electromigration and corrosion, and, finally, be easily patterned by a straight forward process [3].

Most silicon MOS and bipolar integrated circuits now manufactured are metallized with Al or one of its alloys. Aluminum has high conductivity and excellent adhesion to both silicon and silicon dioxide. It also forms low-resistance contacts to p-type and heavily doped n-type silicon [1]. Despite these advantages, aluminum also has some problems in VLSI applications where junctions are shallow. Good step coverage is hard to achieve with aluminum. At the present time, physical vapor deposition is the only method available for depositing aluminum. It is very difficult to get the proper alloy composition to prevent junction spiking and electromigration. It is also difficult to obtain a low resistance contact for high speed switching. Thinner deposits produce higher current densities and higher resistances. Particulate interference, hillock formation and etching difficulty are also other problems which are explained in the literature [1,2].

Molybdenum, on the other hand, provides several advantages over aluminum mainly due to the method of deposition, CVD. With CVD low bulk resistivities, homogeneous films, better surface adhesiveness and smaller grained (large grains cause electromigration) films can be achieved. Also, CVD employs simple equipment and offers the capability of coating a large number of silicon wafers at a time relatively inexpensively. The most important advantage of using CVD molybdenum, however, is its improved step coverage and selectivity.

Molybdenum could be an excellent interconnecting metal because it can be selectively deposited on silicon leaving a silicon dioxide surface uncovered; therefore, the number of process steps can be reduced by eliminating lithography [2]. Lithography is the process of transferring geometric shapes on a mask to the surface of a silicon wafer.

Selective deposition of molybdenum eliminates some of the process steps in VLSI fabrication. The advantages realized by eliminating these process steps could result in a higher product yield and a substantial cost savings. Molybdenum is not without its disadvantages though. Under different sets of conditions, molybdenum was reported to produce high resistivity and porous films, a thermal expansion different from that of silicon and voids formed at the Mo-Si interface due to an undesired reaction with the underlying silicon.

Molybdenum Deposition (Basic Reaction)

Low pressure chemical vapor deposition of molybdenum from MoF_6 takes place by the following reaction:

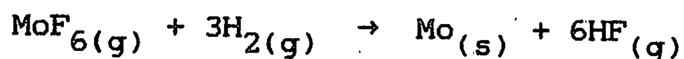

$$MoF_{6(g)} + 3H_{2(g)} \rightarrow Mo_{(s)} + 6HF_{(g)}$$

Another reaction that takes place some time during the hydrogen reduction of MoF_6 is the silicon reduction reaction:

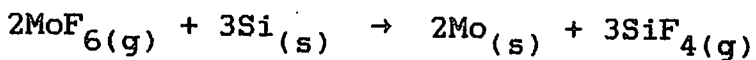

$$2MoF_{6(g)} + 3Si_{(s)} \rightarrow 2Mo_{(s)} + 3SiF_{4(g)}$$

It is known that this reaction must take place sometime during the reaction process because during formation of the Mo layer some Si is consumed (about twice the volume of deposited metal) [25].

Free energy changes shown in Table 1 demonstrate that both reactions are thermodynamically possible [27]. The free energy change for the silicon reduction reaction show that this reaction is more favorable. Although the silicon reduction reaction takes place during Mo deposition, the intent of this research was to observe the hydrogen reduction reaction.

Table 1. Free Energy Changes for the MoF_6 Reaction

$T = 300^oC$	H_2 Reduction	Si Reduction
ΔG^o (kcal/mol)	-65	-218

Hydrogen and Silicon Reduction of Molybdenum Pentachloride

Recent studies involving molybdenum stemmed from its possible use in microelectronics. A variety of molybdenum compounds have been used in studying the potential uses of CVD molybdenum. These include MoF_6, $MoCl_5$ and $Mo(CO)_6$. The literature on molybdenum carbonyl [$Mo(CO)_6$], however, showed this compound to be a poor source of molybdenum because of the incorporation of too much carbon in the films. Carbon-comtaminated films are unacceptable for use in microelectronic applications.

In Mo CVD investigations, molybdenum pentachloride ($MoCl_5$) is probably the most studied compound of molybdenum.

Hydrogen reduction of $MoCl_5$ has been accomplished at several temperatures and pressures in order to investigate molybdenum's possible uses in the production of various electronic components. Studies performed at low pressures of 3-15 torr with variable $MoCl_5$ and H_2 partial pressures and a temperature range of 700-1100 ^{o}C showed that by adjusting the deposition parameters, a thin, dense coating with good adhesion can be produced [15].

A similar study on Mo by the hydrogen reduction of $MoCl_5$ incorporated the same low pressure ranges and partial pressure ranges as the previous discussion but with lower temperatures between 500-800 ^{o}C [9]. This study was performed with the potential application of using the deposited molybdenum as a gate metal source in transitors. Here the deposition rate was thought to be controlled by surface reaction and was proportional to the 3/2 power of hydrogen partial pressure in the region of the surface. The films deposited in this temperature and pressure range had a thickness uniformity for a batch of 25 wafers within 5% and the films were not oxidized.

Molybdenum films deposited from $MoCl_5$ at atmospheric pressure and a temperature near 600 ^{o}C was another area of investigation [8,14]. These films were thick and of large grain size. The main interest in the atmospheric deposition studies was to examine the film resistivities as a function

of the purity of molybdenum chloride, poisoning contaminants and growth rate. Quite pure molybdenum films were found by H_2 reduction of $MoCl_5$ at atmospheric pressures. The factors that increased resistivity were found to be microcrystallinity and metalloid contamination. Impurities were MoO_2Cl_2 and incompletely reduced MoO_2 and MoO. Temperatures above 500 ^{o}C minimized the negative influence of oxygen.

Still another area of investigation using $MoCl_5$ as the source of Mo comes from the application of $MoSi_2$ films. Refractory metal silicides, such as $MoSi_2$, are also being studied as highly conductive interconnect and gate-electrode materials. This silicide ($MoSi_2$) is also being studied as a potential material in reducing the gate dimensions in I^2L (integrated injection logic) circuits [24]. Studies in this area all produced good quality, highly oriented thin films. The films may also be easily chemically dry etched and do not form hillocks. Molybdenum disilicide films are also resistant to HCl, HNO_3, H_2PO_4, H_3PO_4, and HF solutions.

Although hydrogen reduction of $MoCl_5$ produces high purity thin films, there are several disadvantages to this method of deposition. Most of the techniques reported excessive film resistivity [15]. There were also reports of unreasonable amounts of film contaminants [12]. The biggest disadvantage in using $MoCl_5$ is that at temperatures below

150 °C, the chlorides condense on any surface. Molybdenum pentachloride also can not be obtained commercially and special equipment is needed to produce this gas. These last two disadvantages make MoF_6 as the source of Mo much more desirable.

Hydrogen and Silicon Reduction of Tungsten Hexafluoride

Molybdenum and tungsten chemistry is similar enough to expect similar CVD behavior. Tungsten deposition by the hydrogen reduction of tungsten hexafluoride for use in microelectronics is well known [32].

Kinetic work by McConica and Krishnamani, and Broadbent and Ramiller, showed deposition of tungsten from WF_6 is very similar to molybdenum deposition from MoF_6 [28,29]. They found hydrogen reduction of WF_6 to be 1/2 order in hydrogen and zero order in WF_6 with an activation energy of 69000 J/mol (0.71eV) at temperatures from 250 °C to 500 °C and pressures from 0.1 to 10 torr. The preexponential factor was determined by McConica and Krishnamani to be 6.2×10^4 $nm/s \cdot Pa^{0.5}$. McConica's and Krishnamani's investigation also reported the rate limiting step could be either the addition of adsorbed monotomic hydrogen to adsorbed, partially fluorinated tungsten, or hydrogen fluoride desorption. However, Broadbent and Ramiller reported the rate limiting mechanism to be the Krishnamani, and Broadbent and Ramiller, also reported dissociation of H_2 adsorbed on the

surface. McConica and tungsten to have a limiting deposition thickness and structure that was dependent upon initial native oxide characteristics. This condition was observed in the absence of hydrogen, or in other words, limiting depositions were only shown in the silicon reduction reaction. Other studies involving the low pressure chemical vapor deposition of tungsten have reported similar findings [1,8,30,31,32].

Hydrogen Reduction of Molybdenum Hexafluoride

As stated earlier, the information on LPCVD molybdenum from the hydrogen reduction of MoF_6 is very limited. There have been only two very recent studies that have conditions somewhat similar to the research conditions utilized in this research.

In a study by Woodruff, et. al., Molybdenum was deposited by hydrogen and silicon reduction of MoF_6 [26]. The temperature ranged from 200-500 ^oC, the pressure ranged from 2-5 torr. The hydrogen flow rate was 100 sccm and the MoF_6 flow rate range 5-25 sccm. Experiments for this study were carried out in a hot wall, low pressure CVD reactor. The MoF_6 was introduced by bubbling hydrogen through MoF_6.

It was found that the reaction was completely selective against deposition on silicon dioxide. The reaction with

silicon took place at a very high rate and was not self-limiting, in contrast to the analogous reaction between WF_6 and Si. To prevent the silicon reduction reaction with molybdenum and thus the severe etching of silicon, attempts were made to put a capping layer between the silicon and the depositing molybdenum. Films of selective CVD tungsten, and sputtered TiW and Mo were ineffective as barrier films to the MoF_6-Si reaction. More importantly, it was discovered that the Mo films deposited over silicon were high in oxygen content and porous.

A similar study by Lifshitz, et. al., was performed in a hot walled, tubular reactor at a temperature range of 200-400 ^oC and a pressure range of 0.2 to 0.9 torr [25]. Mo films were deposited at these conditions by LPCVD on silicon substrates by the reduction of molybdenum hexafluoride in hydrogen and argon atmospheres. The deposition proved to be extremely selective, with no Mo observed on silicon dioxide. Reduction by both hydrogen and silicon were shown to contribute to the deposition with approximately equal, extremely high deposition rates. No self limiting thickness was observed. Again the main feature of the deposits was extreme porosity - about 30%. The films grew in a loose, open structure which could be easily penetrated by reactant gases. This porosity was used to explain such things as high deposition rates, high resistivity and the continuing reaction of Si with the molybdenum hexafluoride reactant.

The only other existing study of LPCVD Mo by the hydrogen reduction of MoF_6 was performed by Schroff and Delval [8]. This study was not performed using a silicon substrates but rather using various substrates such as copper, stainless-steel and molybdenum. The deposition temperature ranged from 600 to 1100 ^{o}C and the pressure varied from 5 to 760 torr within a H_2/MoF_6 ratio of 1 to 60. This investigation was performed to study the dependence of the deposition thickness on the reaction parameters. The number of defects in the films were measured along with the amount of gaseous impurities, in particular, fluorine. It was found that bubble free coatings were obtained when the H_2/MoF_6 ratio was kept within the range of 3 to 6, the pressure kept below 20 torr and the temperature kept above 700 ^{o}C. Low fluorine content deposits were observed to lead to thermal instability.

<u>Analyses by AES</u>

Auger Electron Spectroscopy (AES) is a technique that may be employed in measuring the quality and quantity of CVD deposits. The technique is based on the Auger process. The Auger process itself is preceeded by an excitation process, which leaves an electron hole in a core level of an element. In this case, the preliminary excitation process is

stimulated by absorption of energy from a primary electron beam. After the excitation process, the core hole can be filled by an electron occupying a higher energy level, that is, either a shallower core level or a valence state. This electron must lose energy in the process and the energy is transferred to another electron. This last electron may receive enough energy to leave the system, thus becoming an Auger electron. Auger electrons are then detected by an analyzer that measures their energy.

AES can be used to conduct a depth profiling of the deposited molybdenum. The equipment used in AES depth profiling is equivalent to a standard Auger spectrometer except for the prescence of an ion gun. The ion gun is used to bombard the surface of the sample with ions of an inert gas, usually Argon. The bombardment removes the surface atoms of the sample at a slow rate [33].

If a quantitative Auger analysis is carried out stage by stage during interruptions in the ion bombardment, the results will give the composition of the sample at different depths with respect to the original surface. The depth of molybdenum on silicon can then be obtained from:

$$z = 3.6 \times 10^{-4} [M/\rho] j_p S.$$

where z equals the erosion rate in µm/hr, M is the atomic weight of the target atom in amu's, ρ is the density of the target in g/cm^3, j_p is the primary ion current density in $\mu A/cm^2$ and S is the sputter yield [33].

The Auger depth-profiling technique is affected by several factors like ion mixing, surface roughness, impurities in the ion beam, residual gas adsorption, oxygen content in the chamber, uneven current distribution, etc. These all contribute to poor depth resolution and accuracy. Further details on AES can be found in the literature [33,34].

Analyses by SEM

A very powerful tool in surface studies is scanning electron microscopy (SEM). This technique enables one to observe and analyze phenomena occuring from a scale of about 50 Å to several centimeters. The scanning electron microscope not only permits analysis of very tiny objects, but also reveals the spatial or structural relationships between components analyzed [35].

In the scanning electron microscope, the surface to be analyzed is irradiated with a finely focused electron beam which is rastered across the surface of the specimen. The types of signals produced when the electron beam impinges on a specimen surface include secondary electrons,

backscattered electrons, Auger electrons, characteristic x-rays, and photons of various energies. Secondary emission electrons are preferred to the backscattered elctrons, as they provide higher contrast due to their enhanced emission in the case of rough surfaces [36]. The detector for secondary electrons is only sensitive to electrons that emerge from the specimen with less than 50 keV of energy [37].

The incident beam of electrons that scan the surface of the specimen is similar to that used in a television tube. A directly synchronized raster pattern is displayed on a cathode ray tube, and the intensity of the moving spot is modulated by the signal from the secondary electron detector. In other words, the brightness at any point on the screen will depend on the strength of the signal from the corresponding point on the specimen. In this way, an image of the specimen surface is built up on the CRT, point by point [38].

In using SEM techniques for film studies, information obtained from the secondary electron images is usually morphological. Morphological studies can be performed in several ways [39]. For deposition of metal (i.e. molybdenum) on a surface, a very useful technique is direct recognition of shape or crystal habit. If the system being analyzed is well known, it may be possible to recognize the

various constituents present and obtain an estimate of their relative size and concentration.

Scanning electron microscopy as a qualitative and quantitative technique is not without its flaws however. The operation of the equipment, the sample preparation and the interpretation of the instrument parameters are all very complicated. A very skilled and experienced technician is required to operate SEM equipment. Other factors that affect SEM results are specimen contamination, multiple scattering, channeling patterns, etc. These are explained in detail by Cocks [35].

Analyses by ESCA

Another technique used in the study of thin films is electron spectroscopy for chemical analysis (ESCA). ESCA, like AES, is a surface sensitive technique. ESCA also analyzes electrons released from a surface by their kinetic energies.

Impinging x-rays on a sample surface cause the emission of electrons by the photoelectric effect. The electrons are analyzed by their kinetic energy, and more importantly, their binding energy. The binding energy is determined by:

$$KE = h\upsilon - BE - \sigma_s$$

where KE is the kinetic energy of emitted electrons, $h\upsilon$ is the photon energy, BE is the binding energy of the electrons and σ_s is the spectrometer work function. The spectrometer work function and photon energy are known entities.

Like Auger electrons, the binding energy of the electrons in ESCA are characteristic of the element that produces them. This makes elemental identification possible. The binding energy also indicates the chemical bonding of an atom. For example, it can tell if an atom is combined with oxygen, flourine or other such impurities. This information aids in providing details on the surface chemistry of a film. Further details on ESCA may be found in the literature [40-44].

In analyzing thin films of molybdenum for possible electronic applications, the purity of the film is very important. ESCA analysis may be used in combination with ion sputtering to analyze successive film depths throughout a layer of molybdenum. Each element or impurity can be analyzed to see what chemical shifts or changes are taking place from the sample surface to the interface. Binding energy values for elements and compounds are tabulated in the literature [44]. From these values and their corresponding spectra, the chemical make-up of a film can be determined and also speculation can be made as to film porosity, resistivity, etc.

Analyses by RBS

Rutherford backscattering (RBS) is another technique used in CVD film analysis. This technique, similar to the previous ones, uses a beam of monoenergetic and collimated alpha particles (He-nuclei) to impinge perpendicularly on a target. This technique incorporates a high-energy beam of charged particles. The particles pass through a series of devices which collimate or focus the beam and filter it for a selected type of particle and energy.

When the high energy alpha particles penetrate the surface of a sample, some particles are implanted in the sample, some particles pass through the sample (in the case of a thin target) and other particles are scattered backwards at angles greater than 90° from the incident direction. These backscattered particles that impinge on the detector generate an electrical signal. This signal is amplified and processed by a computer. The data is then printed out in the form of a spectrum.

As in ESCA and AES, elemental identification is also possible in RBS since it produces spectra that are characteristic of the parent atom. However, the advantage of RBS resides in the speed of the technique, its ability to perceive depth distributions of atomic species below the surface without sputtering (ion sputtering can sometimes modify the sample and lead to erroneous conclusions), and the quantitative nature of the results. Further details on

RBS are available in the literature [45].

RBS in thin film studies is important in analyzing for film purity. Observation of an RBS spectra shows whether a film is pure (clean sharp peaks) or combined with other elements (interdiffusion of peaks). The information provided by an RBS spectra can be used in conjunction with ESCA and AES in confirming the chemical state of a deposited film.

RESEARCH OBJECTIVES

The objectives of this research are essentially two-fold:

1. Study the kinetics of the hydrogen reduction of molybdenum hexaflouride on a silicon surface.

2. Characterize deposited molybdenum films by AES, ESCA, SEM and RBS and compare the findings with those published in the literature.

EXPERIMENTAL EQUIPMENT

The stainless steel reactor system is diagramed in Figure 2. This low pressure chemical vapor deposition (LPCVD) system consisted of the following primary components: the gas flow control system, the reactor and heater, the chamber pressure control system, the pumping system, the trap system and the acid gas detection system. The contact substrate heater used in this system was designed such that the silicon wafer received a uniform heating distribution which is required for obtaining accurate kinetic data.

Gas Flow Control System

Hydrogen (99.9995% pure, Matheson Co.), helium (99.9999% pure, Matheson Co.) and molybdenum hexaflouride (99.9%) pure, SERAC Co.) flows were controlled by MKS type 1259 controllers. All the flow controllers were connected to a MKS 247B four channel readout and power supply unit. The gas flows in each channel were set independently, but could have been set as ratios of one another. The controllable gas flow ranges were 0-101 sccm/min for hydrogen, 0-145 sccm/min for helium and 0-21 sccm/min for molybdenum hexaflouride.

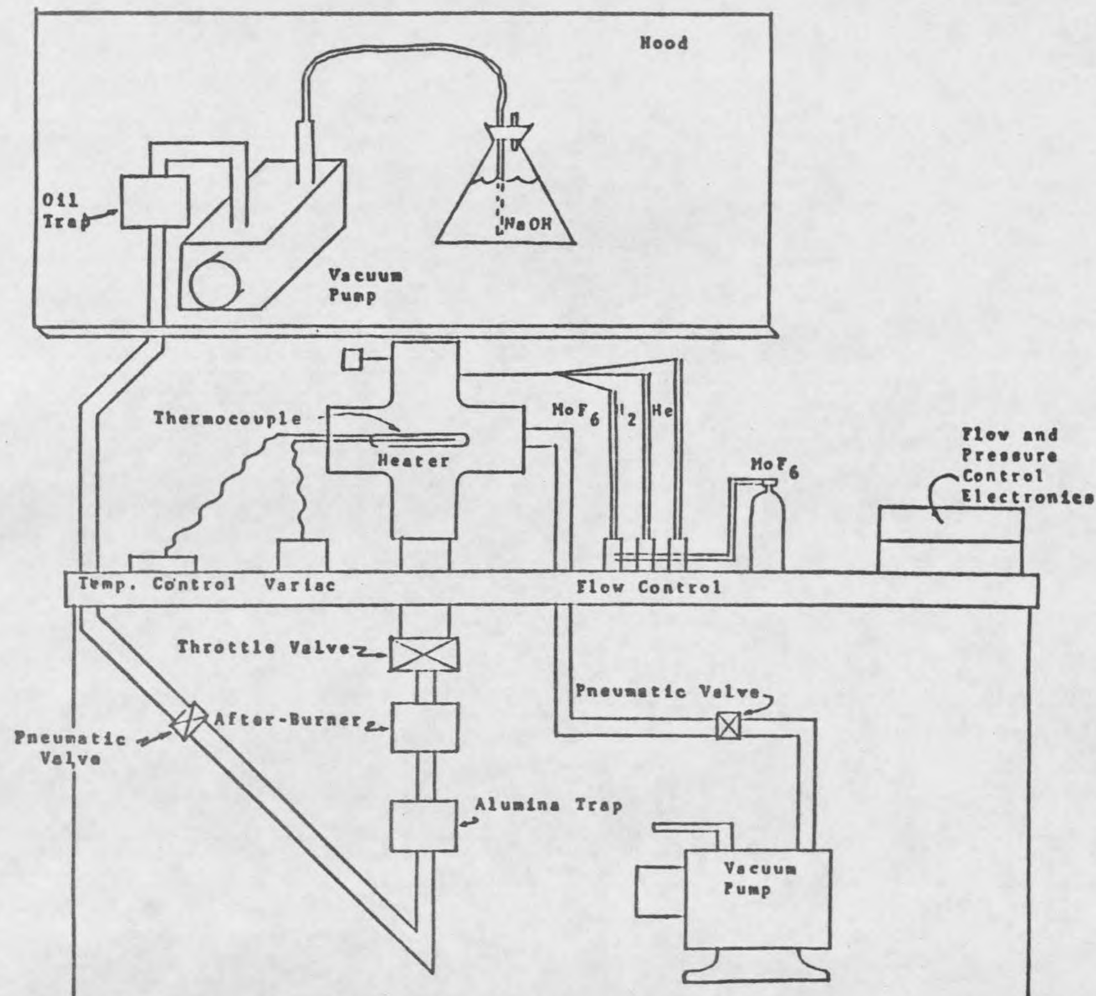

Figure 2. LPCVD Reactor System

Reactor and Heater

The low pressure stainless steel reactor system (Figure 2) was wrapped with fiberglass heat tape to insure that water vapor inside the reactor was kept at a minimum. The reactor was accessed by a flange to which the substrate heater was attached. A 2.5cm X 3.5cm X 5.0cm stainless steel block was used as the substrate holder and heating unit. Centered in this block were four equally spaced ceramic tubes with Ni-chrome wire running through them (Figure 3). The wires were connected in a series arrangement and the total resistance of the system was 2.1 ohms. The leads for the Ni-chrome wires were attached to copper feed-throughs welded in the access flange. These copper feed-throughs were in turn connected to a variac power supply controller. The manually controlled heating arrangement was capable of temperatures up to about 500°C.

Two 1/4" stainless steel rods which were screwed into the feed-through flange acted as the support for the substrate holder. The underside of the substrate holder had two machined grooves for positioning this holder on the rods. The substrate holder was spot-welded to the rods.

Centered at the surface of the substrate holder was the Alumel-chromel thermocouple. The thermocouple wires were attached to larger diameter Alumel-chromel feed-throughs

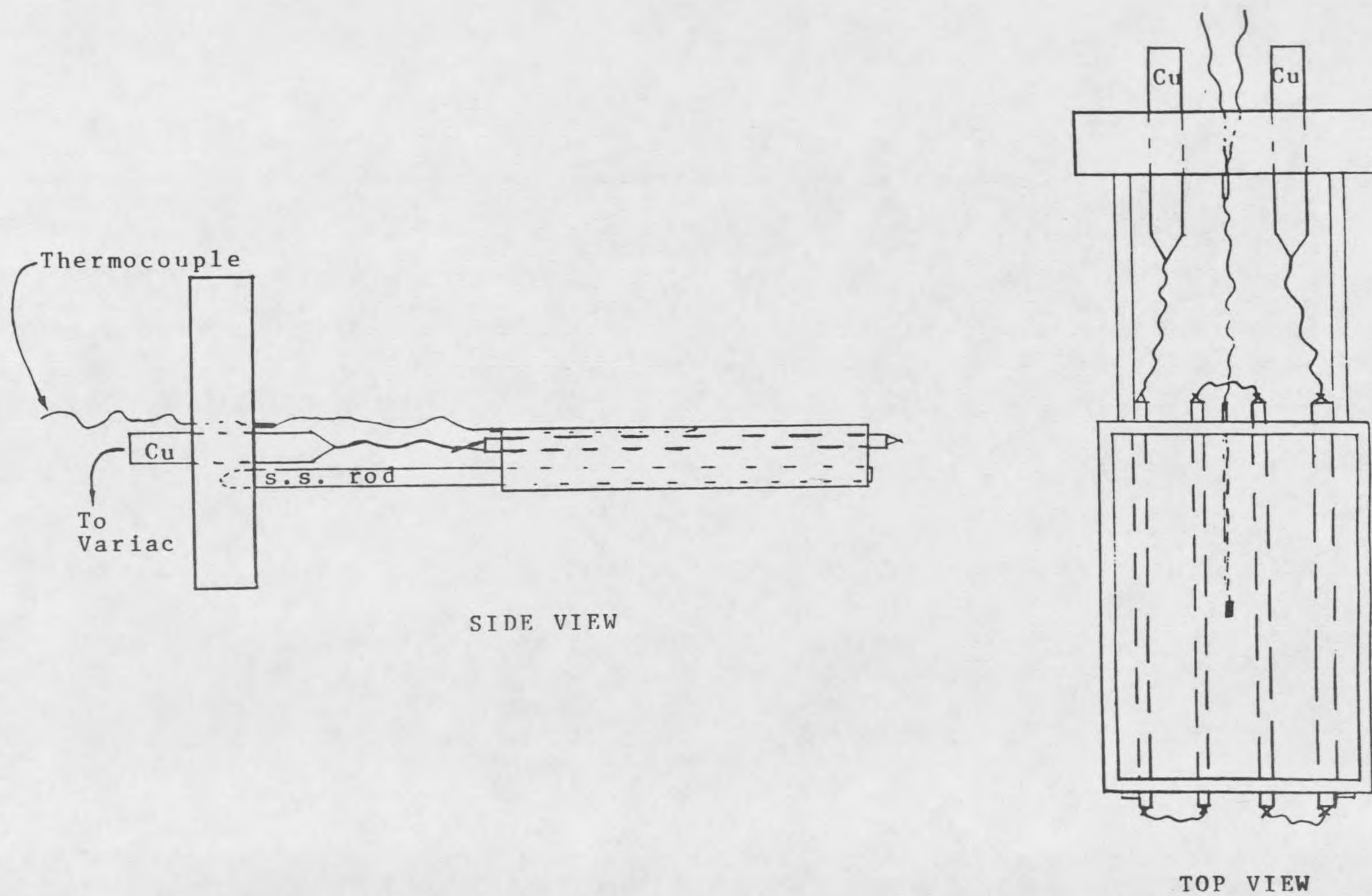

<u>Figure 3.</u> Substrate Heater/Holder for the LPCVD Reactor

which were welded in the access flange. The temperature was recorded by a digital thermometer and was manually controlled by varying the supply voltage through a variac.

Silicon slices were cut to fit into the top grooved portion of the substrate heater/holder.

Pressure Read-Out and Control System

The chamber pressure was sensed by an absolute capacitance manometer gauge, MKS baratron type 222B. This was mounted on top of the reaction chamber. The pressure was displayed on a MKS power supply and digital readout PDR-D-1.

A MKS throttle valve type 253-1-40-1 was quick clamped to the bottom of the reaction chamber. The throttling valve and pressure sensor were interfaced through a MKS exhaust valve controller type 253A. The chamber pressure was controlled by regulating the throttle valve opening and thus the pumping speed.

Pumping System

The pumping system consist of two mechanical roughing pumps connected in parallel. One pump (secondary pump) is a Precision vacuum pump, model D25. The pump sat on the floor below the reactor and evacuated directly from the reaction chamber. This pump has a maximum speed of 1500 l/s (0.88

CFM). The pump was used to achieve the initial vacuum of < 0.02 torr and was isolated from the system by a pneumatic valve during the reaction. The other pump (primary pump) is a Leybold-Heraues, model D4A, which has a maximum speed of 1500 l/s. This pump was located in a exhaust hood and was the pump used during the reaction to exhaust the residual reaction gases.

As stated earlier, the throttle valve was connected to the stainless-steel reaction chamber. Between the throttle valve and the mechanical pump located in the hood were two residual gas traps, an oil trap and a pneumatic valve. The pneumatic valve was a safety feature to protect the pump's oil backstreaming in the lines in case of a power outage. The other mechanical pump also contained this safety feature. Both pneumatic valves were activated by pressurized argon gas and were designed to fail closed.

Acid Gas Detection System

Since HF acid was one of the by-products of the reaction, a sodium hydroxide neutralizing generator was set up in the exhaust hood to neutralize HF gas. When the gases were exhausted from the roughing pump in the hood, they were bubbled through a sodium hydroxide solution where the acid-base reaction took place leaving a sodium flouride precipitate. Phenophthalein was added to the NaOH as an

indicator. The purple indicator turned clear if the solution became acidic.

The purpose of this acid neutralizing station was to provide an indication of how efficient the alumina trap system was in adsorbing the residual HF gas and to protect the pump from this gas. The NaOH solution was made very dilute. The procedure was to change the alumina trap each time a NaOH solution turned clear.

After-Burner and Alumina Trap System

A stainless steel, in-line after-burner and alumina trap were positioned between the throttling valve and the roughing pump located in the hood. The after-burner was a stainless steel can filled with stainless steel shavings. The can was wrapped with ceramic-insulated Ni-chrome wire. Another layer of fiberglass insulation was wrapped around the Ni-chrome wire and secured to the stainless steel can. The Ni-chrome wire was connected to a variac and kept at a constant temperature of around 300°C. Residual MoF_6 from the reactor was reduced on the heated stainless-steel surface.

Two copper rods mounted on a stainless-steel feed-through flange were quick-connected to the side of this after-burner and had spot-welded thermocouples in contact with the stainless shavings in the after-burner. This flange and

the bottom flange (going to the pump) were both cooled to 60°C by cold water running continuously in 1/8" copper tubing. The alumina trap was a stainless-steel can filled alumina. This high surface area alumina adsorbs and neutralizes the HF gas by forming AlF_3.

Chemical Hazards

The safety hazards associated with LPCVD molybdenum mainly dealt with MoF_6, H_2 and HF gases, and also NaOH and NaF solutions.

Fluorides from the reaction could potentially be emitted into the atmosphere or the pumping system. Inorganic fluorides such as MoF_6 and HF are highly irritable and toxic. Molybdenum hexafluoride, when exposed to moist room air, liberates hydrofluoric acid, a very irritating and corrosive substance. Severe exposure will cause rapid inflammation and congestion of the lungs. Skin contact with HF causes irritation, burns and severe pain. The most dangerous effects of skin contact is from HF causing sclerosis of the bones. Sclerosis of the bones is caused by the fixation of calcium by fluorine. Hydrogen fluoride will also corrode and severely reduce the operating life of pumps.

As stated earlier, the after burner reduces residual MoF_6 on the stainless-steel shavings and the alumina trap adsorbs any HF gas on the high surface area alumina. The

sodium hydroxide neutralizing generator is also added as a back-up in indicating the efficiency of the alumina adsorption system. The acid-base reaction that takes place between NaOH and HF produces a NaF precipitate and water. Sodium hydroxide is a toxant and irritant, and can cause severe burns. Sodium fluoride is an inorganic fluoride. The NaF and NaOH solutions may be disposed of by flushing them down the drain with copious amounts of water.

Hydrogen gas is extremely explosive and should not be allowed around any source of ignition. In large quantities in an enclosed area, hydrogen may also cause asphyxiation.

EXPERIMENTAL PROCEDURES

Sample Cleaning

The silicon slices used for deposition were first soaked in dilute HF acid to remove any oxides and cleaned with acetone and methanol to remove organics. All stainless steel flanges, traps and various accessories associated with the reaction chamber were all boiled in distilled water and rinsed with acetone and methanol. The substrate holder was boiled, ultrasonically cleaned and rinsed with acetone and methanol.

Deposition Procedure

A silicon slice was positioned on the substrate heater and placed in the chamber. The reaction chamber and gas lines were then evacuated to approximately 0.02 torr. The gas controller valves were closed and the lines were pressurized with gas to prevent any moisture leak through. During this time the after burner was stabilized at about 300°C and the cooling water was running to protect the after-burner flange. The reaction chamber as well as the gas lines were wrapped with heat tape and kept at a temperature above 70°C to aid in evaporating any remaining water vapor and to keep the MoF_6 from condensing.

The substrate heater was turned on slowly (to protect from thermal shock and breaking of the wires) and stabilized at the deposition temperature (see Table 2). Hydrogen was slowly introduced turning on the exhaust valve controller simultaneously. When the reaction chamber was stabilized at the test pressure and the substrate heater was stabilized at the deposition temperature, the MoF_6 was introduced into the chamber. The residence time of the MoF_6 gas was approximately five seconds. Immediately a timer was turned on and the substrate temperature was manually controlled to within $\pm$ 2°C. Careful attention was given to the color of the NaOH-phenophthalein solution.

At the end of deposition the hydrogen and MoF_6 were shut off. The throttle valve was opened completely and helium was introduced into the chamber to purge the system. While the helium purged the system (for 5 minutes), the substrate temperature was reduced. After purging the throttle valve was closed and helium was introduced into the chamber to cool down the substrate. When the substrate reached a temperature of about 65°C, the chamber was brought to atmospheric pressure with helium and the sample was removed for analysis.

AES Analysis Procedure

When the sample was removed from the reaction chamber, it was labeled and transported to the Montana State

Table 2. Temperature, Time and Partial Pressure Variations for the Kinetic Study of the Hydrogen Reduction of Molybdenum Hexafluoride

time (min)	T (^oC)	P_{MoF_6} (torr)	P_{H_2} (torr)	P_{tot} (torr)
10	250	0.056	0.844	0.900
		0.30	1.00	1.30
		1.50	1.00	2.50
		3.00	1.00	4.00
		0.30	4.70	5.00
		0.30	7.00	7.30
		7.00	1.00	8.00
		0.30	9.70	10.00
5 (*)	300 & 350	0.056	0.844	0.900
		0.30	1.00	1.30
		1.50	1.00	2.50
		3.00	1.00	4.00
		0.30	4.70	5.00
		0.30	7.00	7.30
		7.00	1.00	8.00
		0.30	9.70	10.00
5	400	0.056	0.844	0.900

* Ten, 16 and 20 minute experiments were also run at this partial pressure ratio, total pressure and T = 300 ^oC.

University Physics Department for Auger depth profiling analyses. Each sample piece was cut into 1 cm x 1 cm sections so that each section of the same sample could be analyzed by different methods.

The AES depth profiling scans were performed by a Physical Electronics (PHI 595) scanning Auger microprobe. Each sample was sputtered by an Argon (Ar^+) ion beam for 1/2 to 5 minute intervals. At the end of each interval, the area sputtered by the ion beam was analyzed by AES. The primary electron beam had a voltage of 3.0 keV and a beam current of approximately 0.20 μA. The analyses gave the surface composition after each successive ion sputter. The surface composition data was recorded digitially on a magnetic disc with the use of a DEC PDP 11/04 computer.

In using AES as an instrumental analysis technique, a few problems were encountered. Due to the amount of surface roughness and impurities (oxygen, flourine, carbon) associated with each sample, a constant sputter yield could not be obtained [46]. Without a constant sputter yield, the AES depth equation was invalid.

Realizing these problems, AES was then used on a semi-quantitative and qualitative basis. In other words, even though definite amounts of molybdenum deposited could not be

determined for each sample, relative amounts of molybdenum and impurities present could be determined.

SEM Analysis Procedure

Samples for SEM analysis were taken to the Vetinary Science Department at Montana State University. Samples were cut to be 5 mm x 5 mm in size for a cross-section and surface analyses by SEM. The cutting procedure was performed by scoring the backside of the sample and fracturing along the scored line. The samples were then prepared, processed, and photographed by the operating technician in the department.

ESCA Analysis Procedure

The ESCA scans of the molybdenum deposited samples were performed by a Leybold-Hereaeus x-ray photoelectron spectrometer (L-H EA11). The radiation source was non-monochromatized Mg $K\alpha$ (KE = 1253.6 eV) x-rays.

The ESCA data was recorded both with an analog and digital recorder. A special program developed by XEROX and modified by the Montana State University Physics Department aided in analyzing the ESCA data. This program provided the capability to smooth the data and obtain the kinetic energy locations of the peaks.

Acid Dissolution Procedure

Acid etching was performed by starting with a solution consisting of: 5 ml of H_3PO_4 (85%), 30 ml of HNO_3 (70%), 4 ml of CH_3COOH (99%) and 150 ml H_2O. The solution was contained in a pyrex beaker.

The 1 x 1 cm sample was carefully placed in the acid solution, agitated gently and weighed. The weight was measured on a CAHN 29 automatic electrobalance model number C-29. Each sample was dipped and weighed at 5 minute intervals until there was no significant weight change. The solution was tested for selectivity of molybdenum over silicon and was found to be completely selective.

RBS Analyses Procedure

RBS was performed in the Montana State University Physics Department. The non-commercial instrument incorporated a beam of 1.4 MeV (He nuclei).

RESULTS AND DISCUSSION

Thickness Determination of Deposited Samples

Acid etching produced the values given in Table 3. The etching proved to be a good method in determining the amount of molybdenum deposited. The validity of this technique was checked by measuring the film thicknesses pictured on SEM micrograph cross-sections. The SEM thickness measurements were compared to acid dissolution film thickness measurements and were shown to be in good agreement.

As discussed in the experimental section of this report, AES was used to determine the differing amounts of impurities present in each sample. This was because the sputter yield varied for samples of the same thickness; therefore, the AES depth equation for determining the amount of deposition was not used.

Reaction Kinetics

Figure 4 shows molybdenum thickness versus time at a constant total reaction pressure of 0.9 torr and a temperature of 300°C. The plot indicates a non-linear relationship. The reaction shows a high rate of deposition as time increases (past 15 minutes) and there is no observed self-limiting behavior. The lack of self-limiting behavior has been observed by other researchers, but there has been no report of molybdenum deposition on silicon being non-linear [26]. By using Figure 4 and the Auger analysis of

Table 3. Molybdenum Film Thickness Measurements by Acid Dissolution (for the Kinetic Data).

T (°C)	P_{tot} (torr)	P_{H_2}/P_{MoF_6}	Film Thickness* (nm)
250 (10 min)	0.9	15	22
	1.3	3.3	22
	2.5	0.67	12
	4.0	0.33	69
	5.0	15	57
	7.3	23	60
	8.0	0.14	22
	10.0	32	90
300 (5 min)	0.9	15	53
	1.3	3.3	105
	2.5	0.67	118
	4.0	0.33	264
	5.0	15	139
	7.3	23	185
	8.0	0.14	138
	10.0	32	287
(10 min)	0.9	15	93
(16 min)	0.9	15	170
(20 min)	0.9	15	320

* Thickness measurement results were repeatable within ± 4 nm.

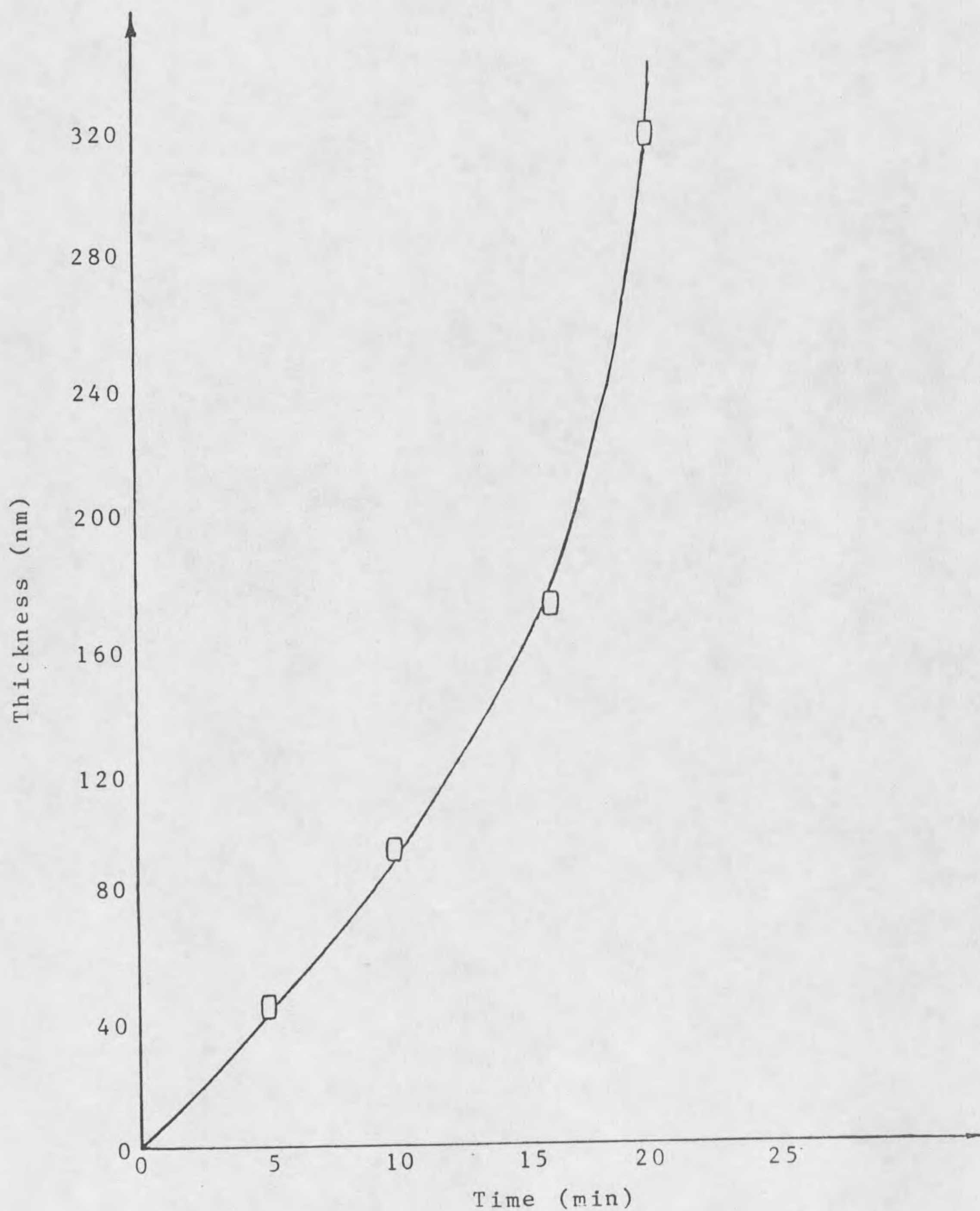

Figure 4. Molybdenum Thickness as a Function of Time at $T = 300\ ^{o}C$ and $P_{tot} = 0.9$ torr

samples deposited at 250 °C, 300 °C and 350 °C, it was determined that ten minutes of reaction time provided sufficient thicknesses of 10 nm or greater for the 250 °C samples and that five minutes of reaction time also provided sufficient thicknesses of 10 nm or greater for the 300°C and above samples. These times were also short enough for a linear initial rate to be used in analysis.

Figure 5 shows an Arrhenius plot for reciprocal temperature versus r (rate of deposition) for total pressures of 0.9 and 5.0 torr and for total deposition times of five and ten minutes. The hydrogen to MoF_6 ratio was kept constant at 15:1. A slope was calculated from each total pressure curve. From these values an average activation energy of 76,000 ± 1500 J/mol was determined.

Order of Reaction

The reaction order with respect to hydrogen was determined as a function of the partial pressure of MoF_6. The partial pressure of MoF_6 was kept constant while the hydrogen partial pressure varied from 1.0 to 9.7 torr within a temperature range of 250-350°C. Figure 6 shows the plots of ln r (rate of deposition) as a function of ln P_{H2} (partial pressure of hydrogen). The reaction order with respect to hydrogen was determined from the slope of these plots. The average value of the reaction order with respect to hydrogen was determined to be 0.5.

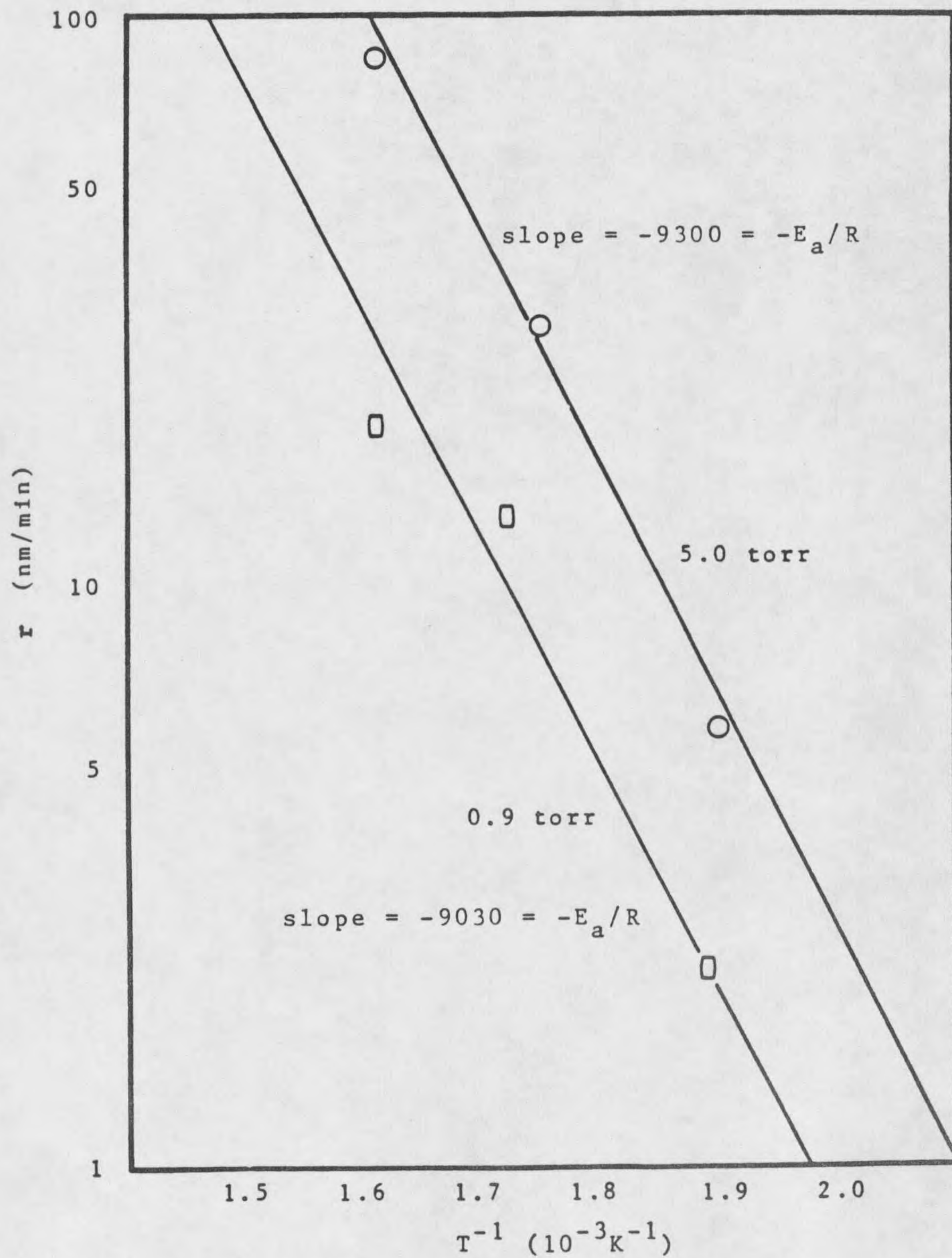

Figure 5. Arrhenius Plot

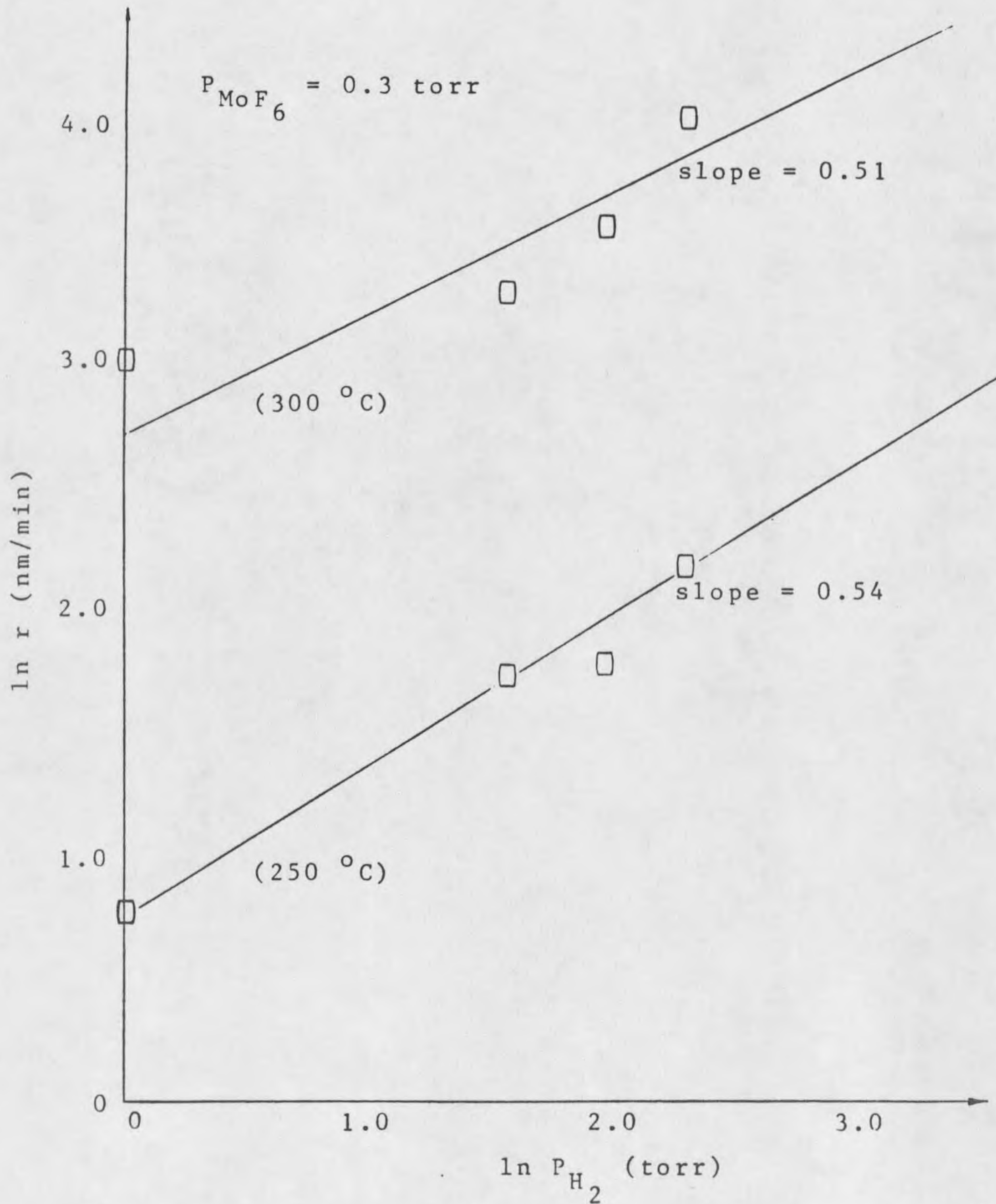

Figure 6. Plot for Determining Order of Reaction With Respect to Hydrogen Partial Pressure

Similarly, the reaction order with respect to MoF_6 was determined as a function of the partial pressure of hydrogen. The hydrogen partial pressure was held constant at 1.0 torr while the MoF_6 partial pressure varied from 1.5 to 7.0 torr within a temperature range of 250-350^oC. Figure 7 shows the results of the ln r (rate of deposition) plotted as a function of ln P_{MoF_6} (partial pressure of MoF_6). The order of reaction with respect to MoF_6 was determined from the slope values. The values obtained had a slight variance and were statistically averaged. From the statistical average, a reaction order of 0.0 with respect to MoF_6 was inferred.

Rate Equation

For all of the experimental runs, the pre-exponential factor k_o was calculated knowing the activation energy, order of reaction and the reaction rate at each temperature from:

$$k_o = r/(e^{-E/RT})(P^{0.5}_{H_2}P^{0}_{MoF_6})$$

where

r = Reaction rate, (nm/s)

k_o = Pre-exponential factor, (nm/s/torr$^{0.5}$)

P_{H_2} = Partial pressure of hydrogen, (torr)

P_{MoF_6} = Partial pressure of MoF_6, (torr)

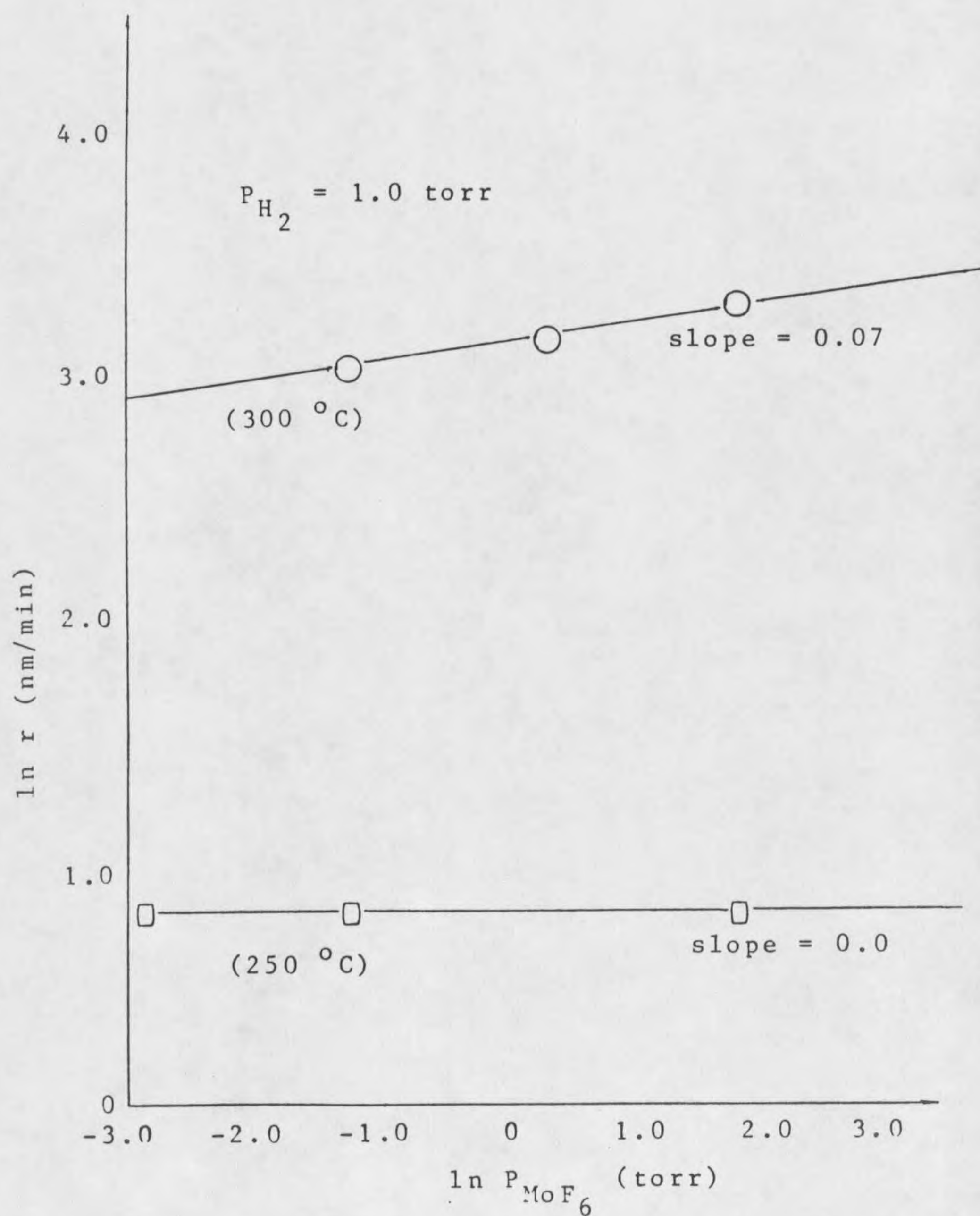

Figure 7. Plot for Determining Order of Reaction With Respect to Molybdenum Hexafluoride Partial Pressure

E = Activation energy of the reaction, (J/g-mol)

R = Universal gas constant, (J/g-mol·K)

T = Temperature, (K)

A statistical average of all the k_o values was performed and k_o was determined to be $2.02 \times 10^6 \pm 1.2 \times 10^6$ nm·s^{-1}·$torr^{-0.5}$. Using k_o and the previous rate expression, the growth rate of molybdenum in units of nm/s due to hydrogen reduction of MoF_6 can be expressed as:

$$r = 2.02 \times 10^6 \, e^{(-9140/T)} \, P^0_{MoF_6} \, P^{0.5}_{H_2}$$

Characterization of Molybdenum Films

Figure 8 shows an AES depth profile of a sample formed at 4 torr of total pressure and a substrate temperature of 300 °C. This sample had a 5% oxygen content and an 85% molybdenum content with silicon, carbon, and fluorine comprising the other 10% of impurities (at molybdenum's highest peak value). This profile displays one of the better depth resolutions.

Table 4 shows the relative amounts of molybdenum and impurities present in samples for which depth profiles were conducted. Here, oxygen is shown to be the highest percentage impurity in the samples. The rows which do not show impurity percentages were poor quality deposits and had

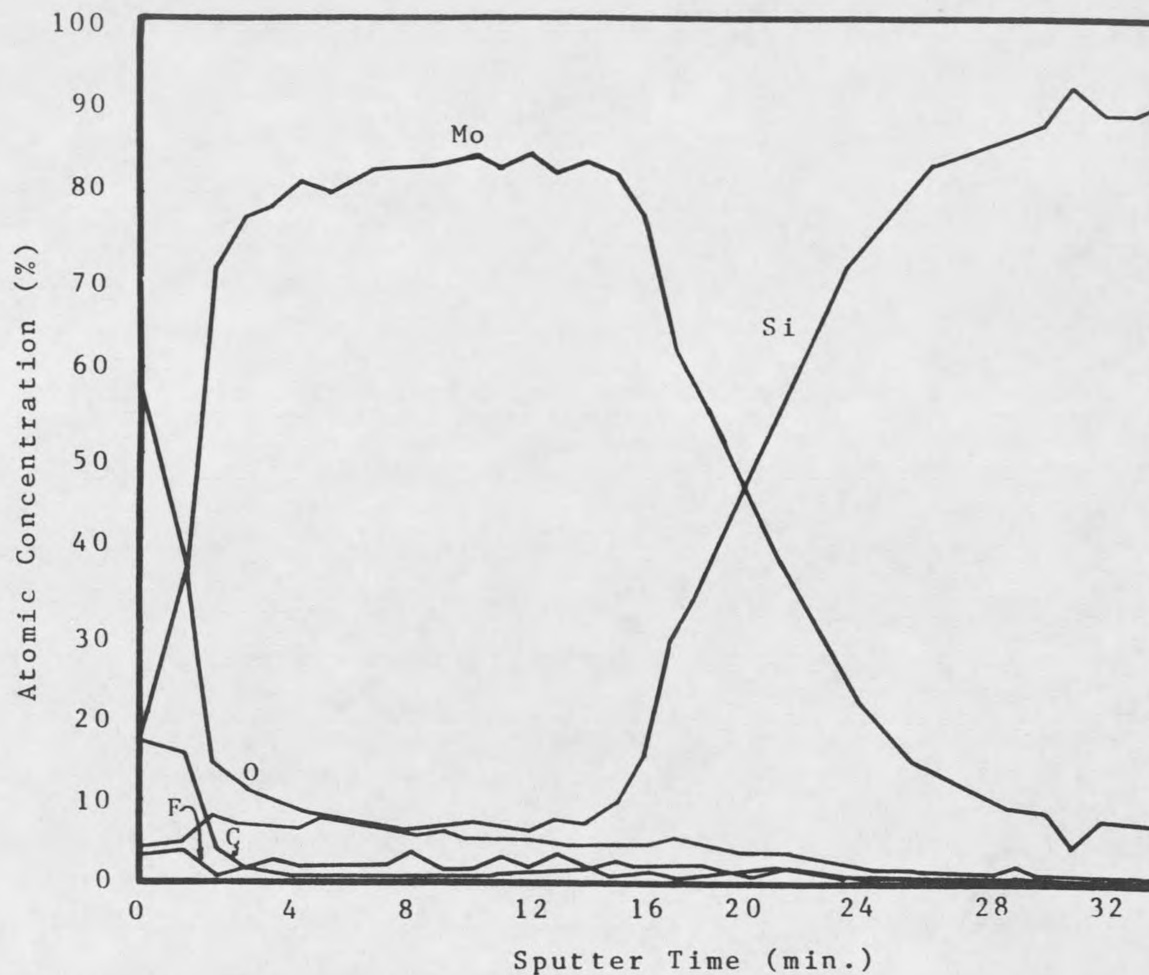

Figure 8. AES Depth Profile of a Mo Film Deposited at $T = 300\ ^{o}C$ and $P_{tot} = 4$ torr

Table 4. Relative Molybdenum Film Impurities from AES Depth Profiles at Molybdenum's Highest Peak Value

T (°C)	P_{tot} (torr)	Rel. % Mo	Rel. % O	Rel. % Si	Rel. % F	Rel. % C	Est. Error ±
250	0.9	55	18	17	3	7	5
	1.3	--	--	--	--	--	
	2.5	--	--	--	--	--	
	4.0	70	13	10	4	3	4
	5.0	--	--	--	--	--	
	7.3	61	28	6	3	2	5
300	0.9	71	14	8	3	4	4
	1.3	61	22	6	7	4	5
	2.5	58	18	16	3	5	6
	4.0	85	5	7	1	2	3
	5.0	--	--	--	--	--	
	7.3	--	--	--	--	--	
350	0.9	66	18	8	6	2	5
	1.3	--	--	--	--	--	
	2.5	--	--	--	--	--	
	4.0	40	27	20	7	6	7
	5.0	58	20	5	13	4	6
	7.3	--	--	--	--	--	
400	0.9	77	11	6	4	2	5

to be repeated. The poor quality deposits had a very high oxygen content, a poor surface color and a film that flaked away. Due to the insufficient time available, the molybdenum films that were deposited again were not analyzed by AES.

In a study performed by Lifshitz, et. al., excess oxygen was determined to be dependent upon the temperature at which the reactor was opened to air; however, the reactor in this study was never opened to air at a high temperature [25]. Oxygen content was also speculated to be dependent upon reactor cleanliness. When the reactor was baked at 400 ^{o}C before the reaction, the films were of better purity.

An ESCA analysis of a molybdenum film deposited at 350°C and 5 torr yields the oxygen 1s band in Figure 9(a). The figure shows two overlapping bands and indicates the presence of oxygen throughout the film. The high binding energy (BE) band indicates the presence of adsorbed oxygen and the low BE band indicates metal oxide. Although film porosity could not be observed with the instrumental techniques available, other investigators attributed the presence of adsorbed oxygen to the film porosity [25,26]. The porosity of the film also explained such phenomena as extremely high deposition rates, uninterrupted Si reduction, uniform oxidation and high resistivity films [25]. In similar studies with tungsten, silicon reduction was shown to reach a limiting film thickness [28].

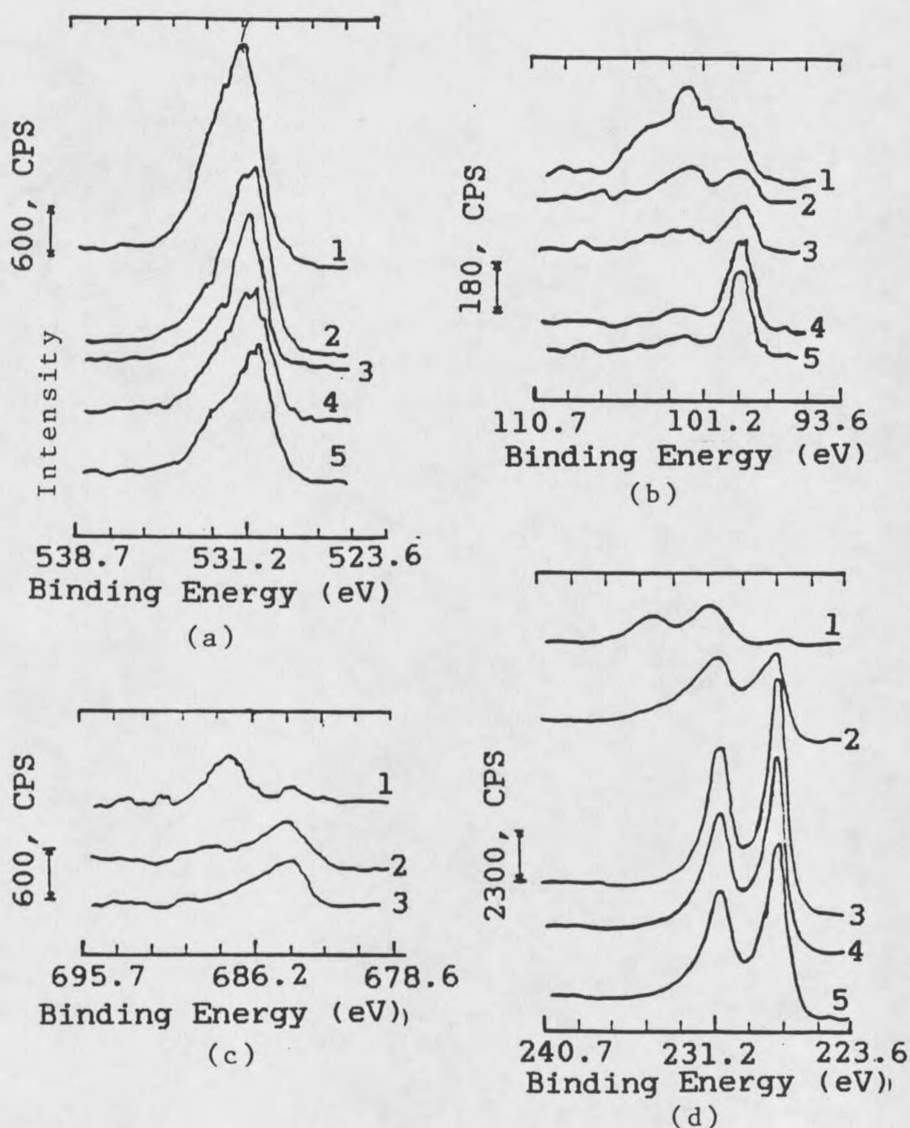

Figure 9. ESCA Spectra for a Mo Film Deposited at T = 350 °C and P_{tot} = 5 torr. a) O 1s band, b) Si 2p band, c) F 1s band, d) Mo 3d band. 1) as received, 2) after 120 seconds sputter etching, 3) after 1.2 hours sputter etching, 4) after 1.83 hours sputter etching and annealing at 350 °C under vacuum for 600 seconds, 5) after additional annealing at 800 °C for 600 seconds.

Adsorbed oxygen in the films was also combined with silicon as seen by the silicon 2p bands in Figure 9(b). The highest BE shoulder to the left has energy which corresponds to oxidized silicon. The peak in the middle has energy close to that of silicon oxy-fluoride. The lowest energy shoulder on the right is that of elemental silicon. After sputtering for 1.2 hours, the oxidized silicon and silicon oxy-fluoride peaks are greatly diminished. An additional 0.63 hours of sputter-etching reduced the intensity of these peaks even more. Considering the decreases in impurities as the interface is approached, this figure suggests that the film is more porous at the surface than at the interface.

The fluorine 1s spectra in Figure 9(c) shows the same trend as the silicon spectra. The two bands in the figure show oxy-fluoride (high BE) and metal fluoride (low BE). Again, the oxy-fluoride peak is diminished as the interface is approached. Schroff, et. al. [11] and Chin, et. al. [30], believe that to obtain a higher quality film and reduce fluorine content, it seems reasonable to work at high temperatures, at high ratios of H_2 to halide, at low pressures and with no moisture or carbon.

The carbon can come from the oil of the mechanical pump or from the atmosphere as volatile hydrocarbons or CO_2 and CO adsorbed on the pore surface.

It is difficult to speculate informatively about the molybdenum spectra in Figure 9(d). The only trend noticeable is that the Mo spectra is asymetric toward higher binding energies. The shift toward higher binding energy suggest that some metal-oxides are formed, probably as thin oxide layers on the pore surfaces. Since there was essentially no source of oxygen in the reactor (except for maybe a minute amount adsorbed on the reactor walls), the large amount of oxygen in the Mo layer would have to be incorporated after removal from the reactor.

Impurities may also be seen by analyzing the surface scans of a deposited film. Figures 10 and 11 show surface SEM micrographs of some of the samples. Figure 10 depicts a film formed at a total pressure of 0.9 torr and a temperature of 400°C and displays the best surface smoothness and the fewest amount of "bubbles". Figure 10 was deposited at the highest temperature and the lowest pressure. Figure 11 was deposited at a low temperature (250°C) and a relatively low total pressure (2.5 torr). The deposit depicted by Figure 11 showed more surface bubbles than the deposited pictured in Figure 10.

The surface micrographs show bubbles to decrease with increasing temperature. Bubble formation involves a number of processes. Some authors attribute the presence of

Figure 10. SEM Surface Micrograph of a Mo Film Deposited at $T = 400\ ^{o}C$ and $P_{tot} = 0.9$ torr

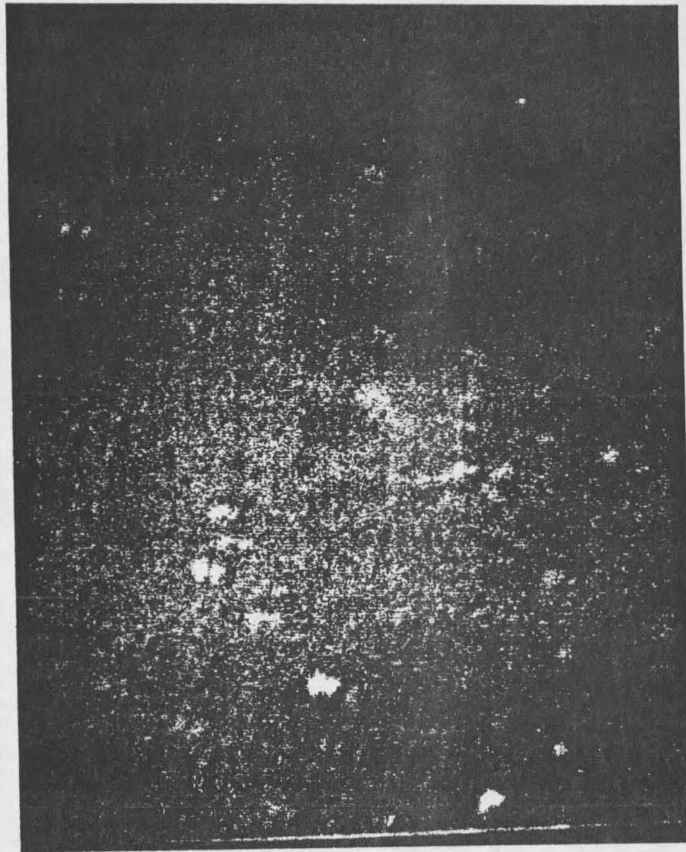

Figure 11. SEM Surface Micrograph of a Mo Film Deposited at $T = 250\ ^{o}C$ and $P_{tot} = 2.5$ torr

bubbles to flourine impurities in the deposits, while the most widely accepted hypothesis is that gas atoms are trapped in the crystal lattice in the supersaturated state during deposition [47]. Shroff and Delval explain bubble growth as follows:

> gas atoms move through the lattice and form tiny clusters which precipitate as bubble nuclei; further expulsion of gas from the lattice cause the individual bubbles to grow and creates more bubbles, the coalescence rate increasing with increasing temperature [8].

Figure 12 shows an SEM micrograph of a surface deposited at 300 ^{o}C and 1.3 torr. Figure 12(a) is before sputtering and Figure 12(b) is after sputtering the surface for 1/2 hour. The film shown in Figure 12 has a smooth surface, and after sputtering not much change in uniformity is observed.

Figure 13 shows a SEM micrograph of a film deposited at 250°C and 7.3 torr. This film was also sputtered for a 1/2 hour. The high pressure low temperature formation conditions initially produced a rough surface and after sputtering (Fig. 13(b), the surface showed a non-uniform condition or the presence of white and dark spots. The film shown in Figure 12 was formed at a higher temperature and lower total pressure than Figure 13. From the surface micrograph analyses, Figure 12 shows a better deposit; however, film thickness and uniformity are two other

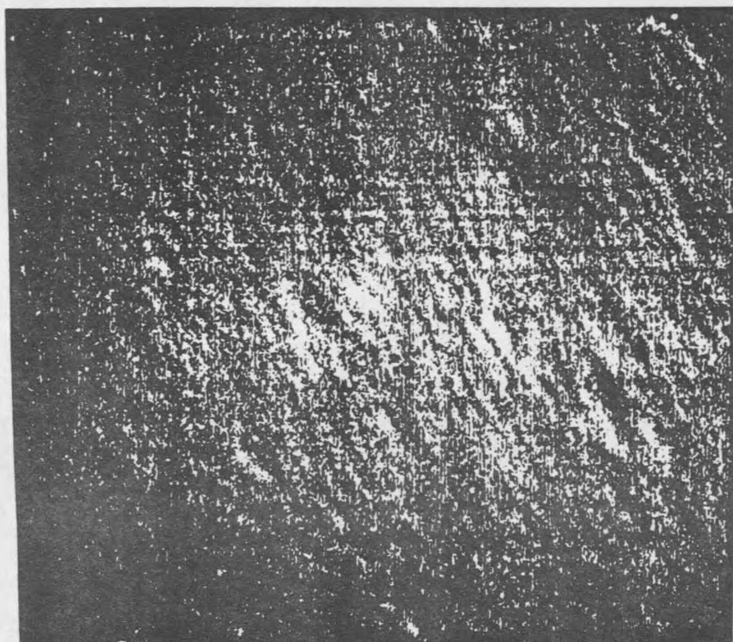

1KX

(a)

1KX

(b)

Figure 12. SEM Surface Micrograph of a Mo Film Deposited at $T = 300\ ^{o}C$ and $P_{tot} = 1.3$ torr

(a) as received;
(b) after sputter ethcing for 0.5 hours

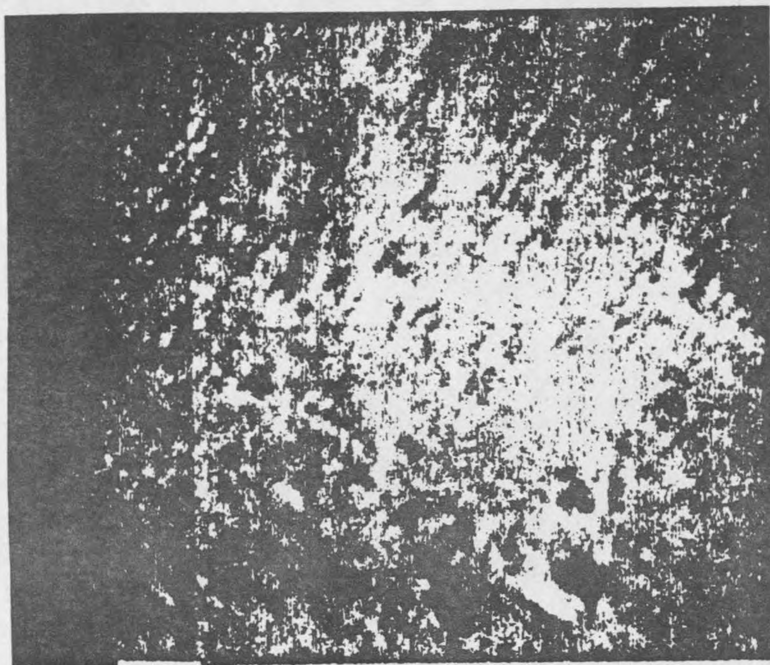

1KX

(a)

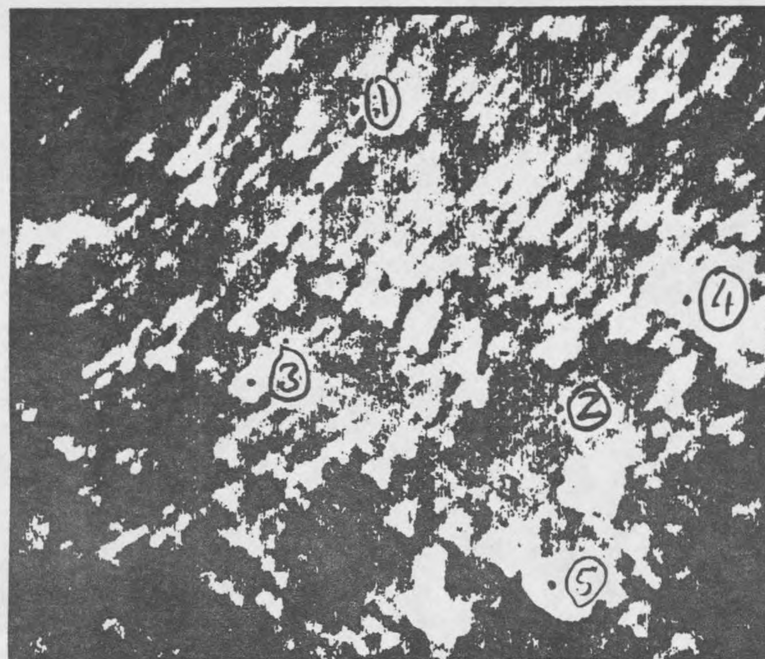

1KX

(b)

Figure 13. SEM Surface Micrograph of a Mo film Deposited at $T = 250\ ^{o}C$ and $P_{tot} = 7.3$ torr (Numbers 1-5 are for AES Point Studies)

(a) as received
(b) after sputter etching for 0.5 hours

important parameters that dictate the quality of a deposited film. The white and dark spots seen in Figure 13 were analyzed for their composition by AES. The white spots were shown to be concentrated in molybdenum and the dark spots concentrated in silicon.

Figure 14 shows a SEM micrograph of a film formed at a total pressure of 5 torr and a temperature of 350°C. Figure 14(b) was obtained after sputtering for one hour and Figure 14(c) after sputtering for 2 hours. If Figure 14(b) and 14(c) are closely observed, a change in the shading of the surface after continued sputtering is noticed. Figure 14(c) also

shows that the molybdenum-silicon mixture depicted by the white and dark spots extends throughout the deposited film and close to the interface.

Points 1 and 4 in Figure 14 were analyzed by an AES elemental analyses. Figures 15 and 16 show the result. The spectra for the dark spot (1) gives a strong peak at 92 eV for Si. The white spot (4) gives strong peaks at 186 and 222 eV, which are the doublet peaks of molybdenum. This spectra also shows moderately strong peaks at 509 eV and 92 eV depicting the presence of oxygen and silicon. Although the Auger scans detect the presence of oxygen, silicon and molybdenum, it does not provide information as to how these elements are combined (i.e. metal oxides, molybdenum silicides, etc.).

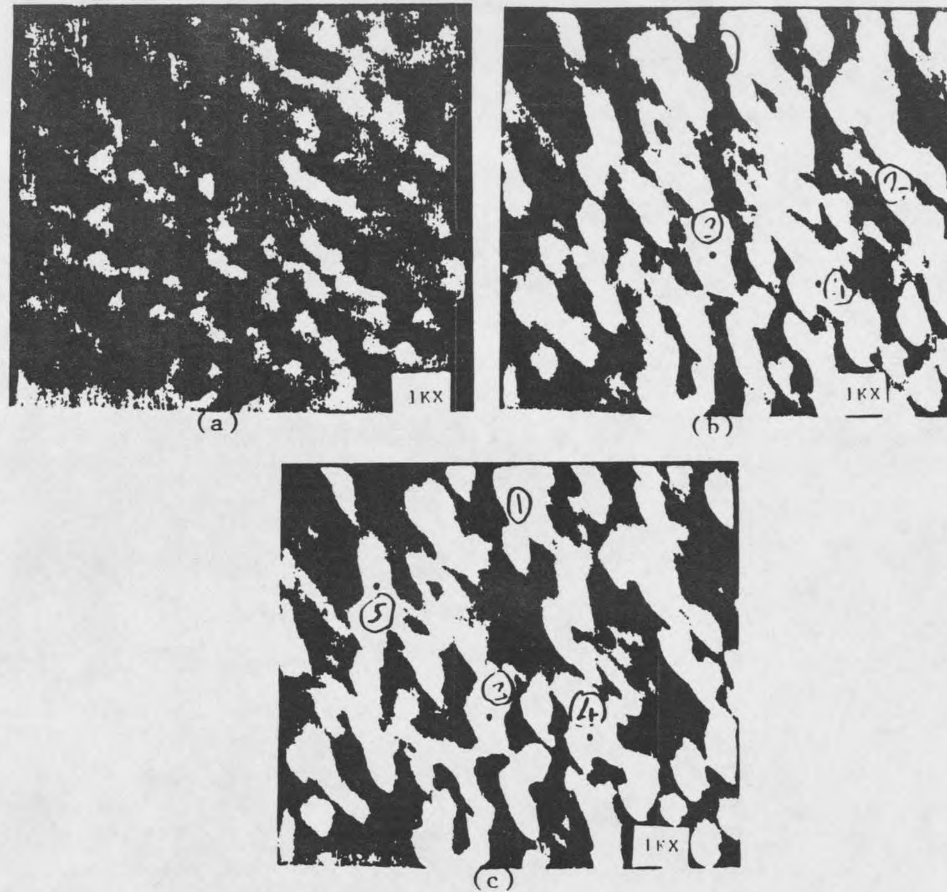

Figure 14. SEM Surface Micrograph of a Mo Film Deposited at $T = 350\ ^{o}C$ and $P_{tot} = 5$ torr (Numbers 1-5 are for AES Point Studies)

(a) as received;
(b) after one hour of sputter etching;
(c) after two hours of sputter etching

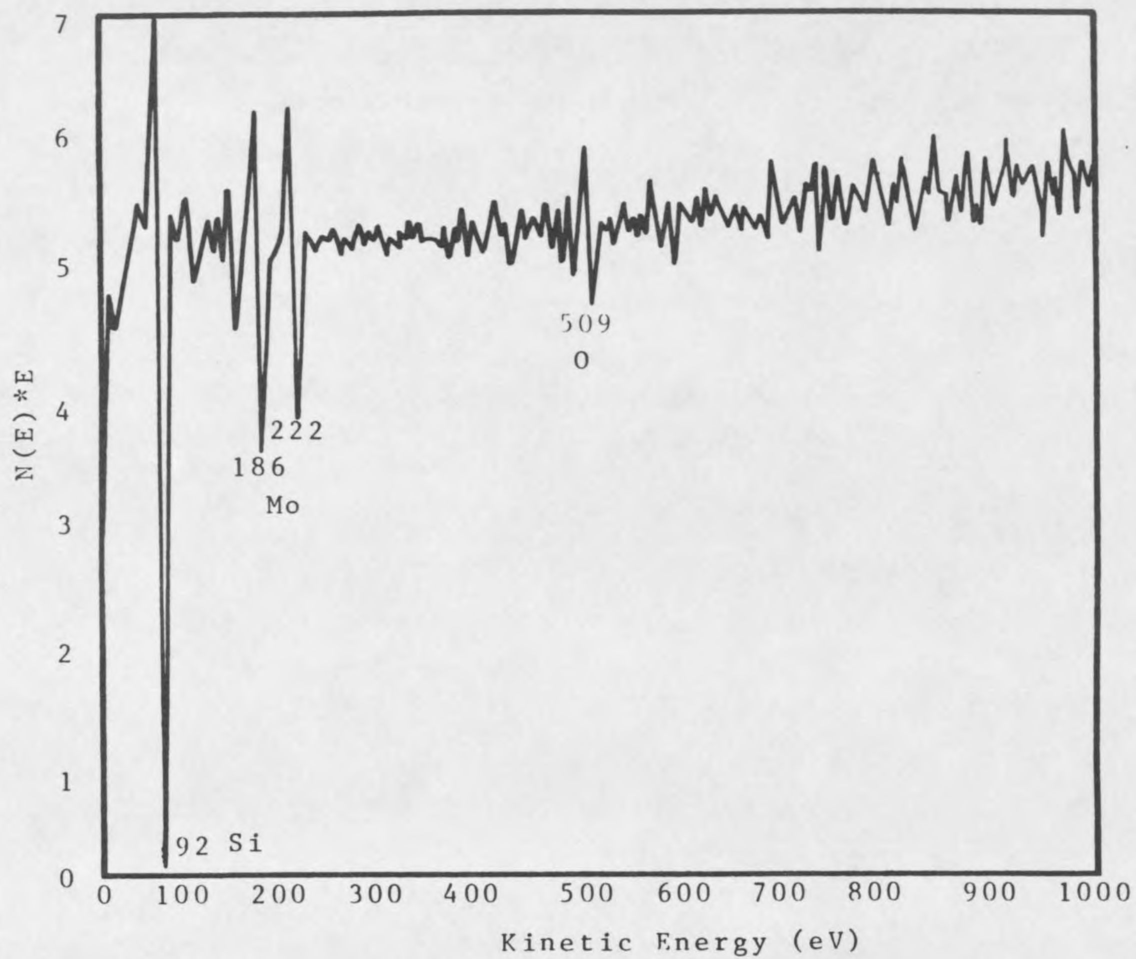

Figure 15. AES Elemental Point Scan of the Surface in Figure 14 (b); point 1

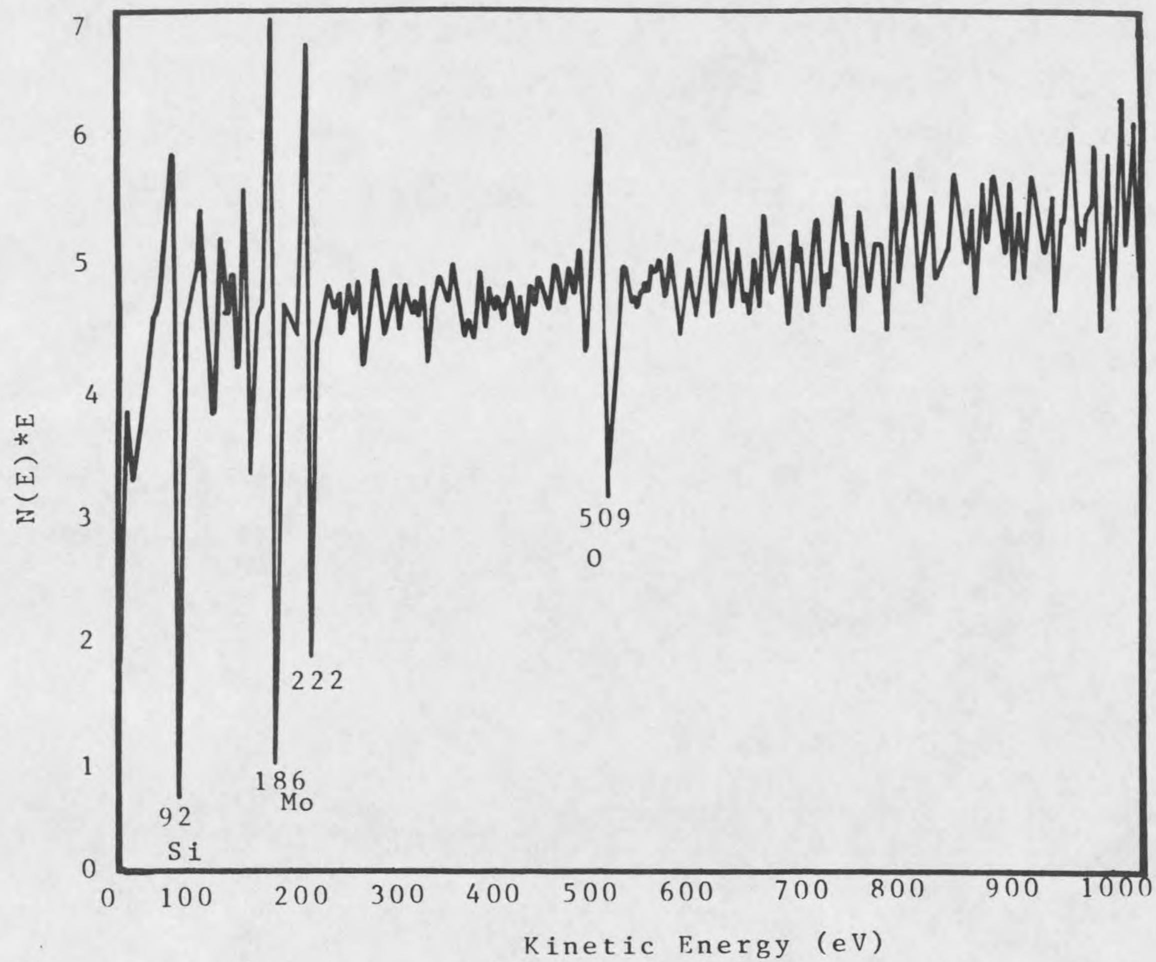

Figure 16. AES Elemental Point Scan of the Surface in Figure 14 (b); point 4

The presence of silicon on the surface of a molybdenum film can also be seen by analyzing the Rutherford backscattering spectra. Figure 17(a) shows the spectra of a molybdenum film deposited at $350^{\circ}C$ and 5 torr superimposed on the spectra of a molybdenum film deposit at $300^{\circ}C$ and 0.9 torr (b). The high intensity peak at the right corresponds to that of molybdenum and the low intensity peak on the left is that of silicon.

Figure 17(b) displays a sharp molybdenum peak with no overlap into the energy range of the silicon peak. The peak of figure 17(a) however shows some interdiffusion of the silicon into the molybdenum or vice versa. In this case, even though figure 17(a) is the higher temperature deposit, the high pressure (5 torr) associated with the deposition conditions may be enough to decrease the purity of the sample.

Schroff reports that higher pressure deposits are full of microdefects [11]. This is because growth is faster in the direction perpendicular to the surface than in the direction parallel. At low pressures the number of gas molecules is small, consequently so is the number of defects.

A SEM cross-section of the film above (Fig. 17(a)) deposited at $350^{\circ}C$ and a total pressure of 5 torr is shown

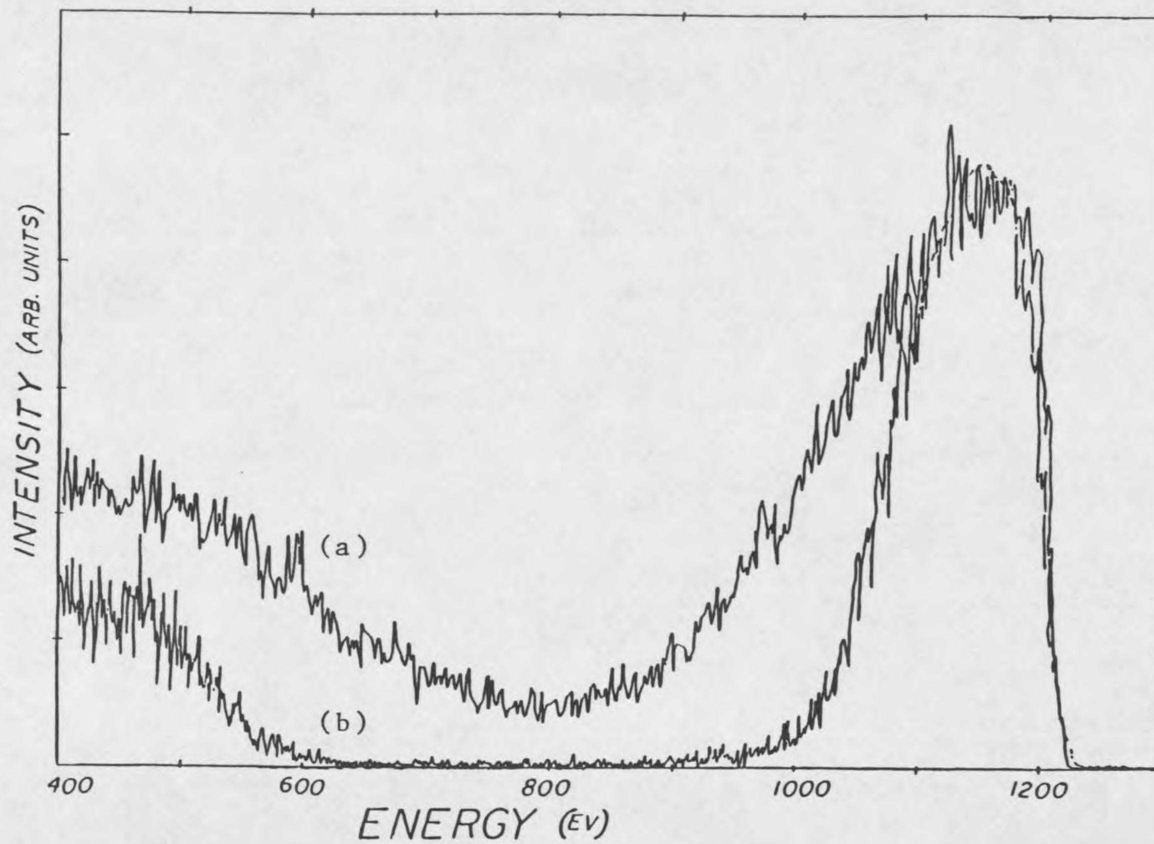

Figure 17. Rutherford Backscattering Scan of Mo Films

(a) Deposited at $T = 350\ ^{o}C$ and $P_{tot} = 5$ torr;
(b) Deposited at $T = 300\ ^{o}C$ and $P_{tot} \cong 0.9$ torr

in Figure 18. The high pressure deposition conditions, again, may explain the rough interface and non-uniform condition of this film. It also appears that silicon reduction of the MoF_6 could attribute to the interface roughness.

Figure 19 shows SEM cross-sections of two different sections of a sample deposited at a high temperature (400^oC) and a low pressure (0.9 torr). In figure 19(a), the 2.25 micron sample shows good adhesion with a relatively smooth interface. The film in figure 19(b) shows a rough interface. The roughness of this interface again suggest some silicon reduction may have occurred. The middle section of this figure shows a film characteristic called "wormholeing". The wormholeing may have been caused by the deposition or possibly from fracturing the sample for SEM analysis.

For this research study, high temperature, low pressure films produced the best quality films. Previous literature on tungsten and molybdenum deposition also supports this finding [8,11]. The major drawback of the molybdenum films however is their extreme porosity. Phenomena such as uninterrupted Si reduction and uniform oxidation of the films were reportedly due to the reactant and product gases continually diffusing through the open porous structure of the deposited films [25]. Film porosity was observed both in hydrogen and silicon reduction of MoF_6 and most

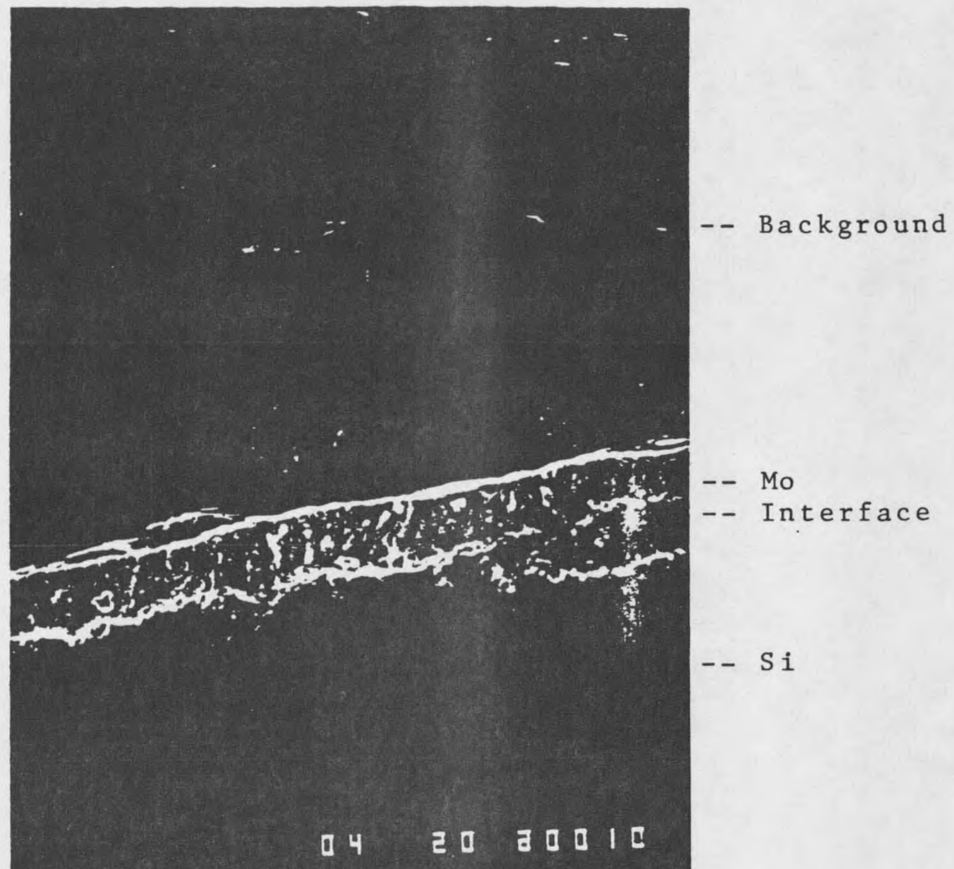

Figure 18. SEM Cross-Section of a Mo Film Deposited at $T = 350\ ^{o}C$ and $P_{tot} = 5$ torr

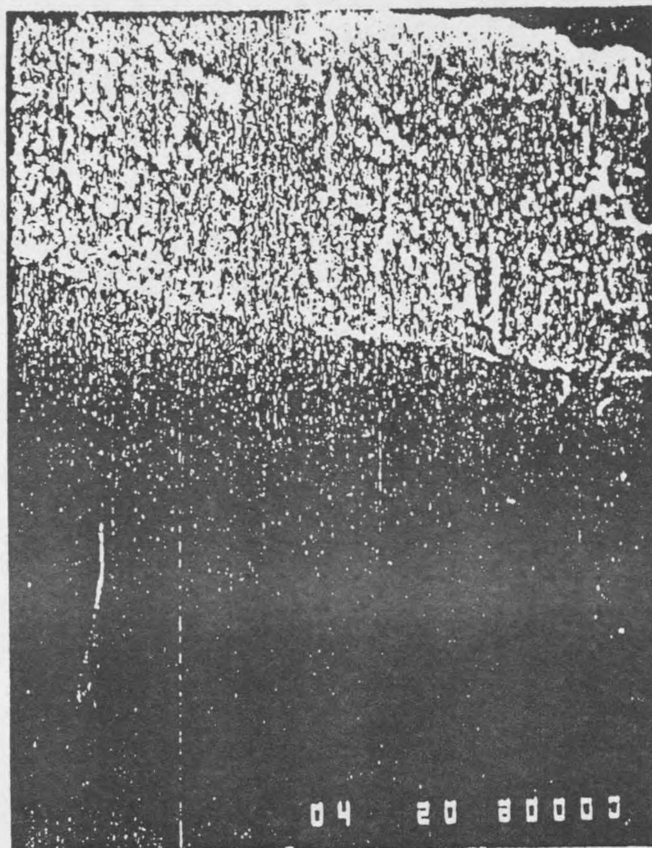

(a)

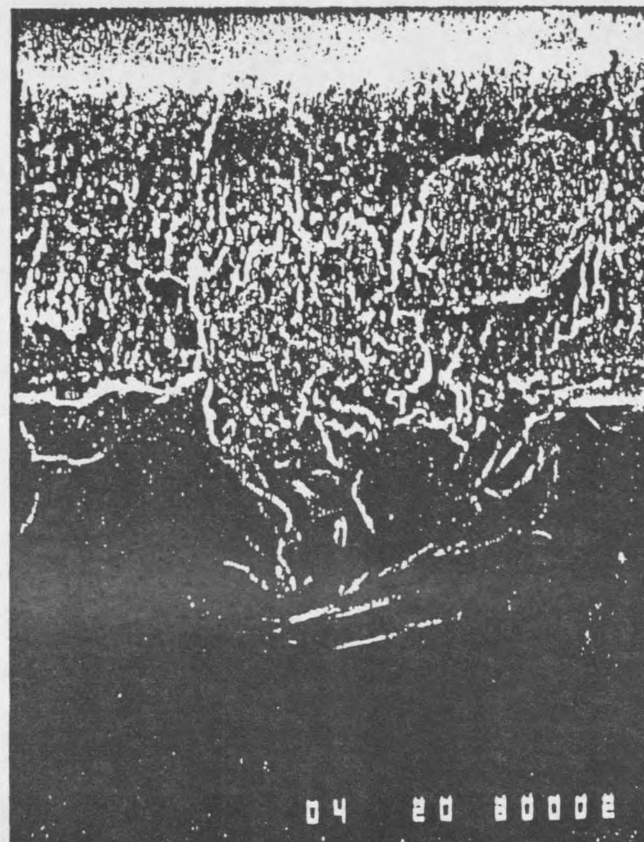

(b)

Figure 19. SEM Cross-Section of a Mo Film Deposited at $T = 400\ ^{o}C$ and $P_{tot} = 0.9$ torr

(a) smooth interface
(b) rough interface with wormholeing

recently in tungsten films by silicon reduction [48]. Tungsten and molybdenum films showed similar characteristics when analyzed by SEM. SEM cross-sections showed W-Si interfaces to be rough, with characteristic protusions and wormholes when tungsten was deposited by silicon reduction [25]. Although the results of the most recent experimenters seem similar to the results found in this experiment, a major difference is that Lifshitz, et. al. [25] and Woodruff, et. al. [26] used a hot-wall reactor instead of a substrate heater.

LPCVD of tungsten and molybdenum also reportedly produced high resistivity films [25,26]. This again was explained by the high porosity of the films. The best molybdenum film resistivity was reported to be 60 μΩ·cm, which is an order of magnitude higher than bulk molybdenum [25]. In this study, a molybdenum film deposited at a total pressure of 0.9 torr and a temperature of 400°C produced a resistivity of 20 μΩ·cm. A comparison of the resistivities of most of the other samples films was unattainable. The other films were not of sufficient thickness or uniformity to be within the accuracy range of the four-point probe which was used for determining resistivities. Other films ranged between 2 μΩ·cm to several hundred μΩ·cm. In general, low pressures favored lower film resistivity.

SUMMARY AND CONCLUSIONS

The objective of this research was to examine molybdenum CVD films by AES, RBS, ESCA, and SEM, and to study reaction kinetics for the hydrogen reduction of MoF_6. The significant findings of this investigation are as follows:

1. Examination of the CVD molybdenum films showed oxygen content in some films to be as high as 28%. Since there was essentially no oxygen in the chamber during the reaction, oxygen was assumed to be incorporated in the sample after removal from the reaction chamber. The incorporation of oxygen and impurities in a sample inferred a porous deposit. This porosity could also explain the high resitivity of molybdenum LPCVD films.

2. Although there was no absolute trend between the deposition parameters and the purity and quality of a deposited film, high temperatures and low pressures seem to produce the best results.

3. A kinetic study showed the hyrogen reduction of molybdenum hexafluoride to be 1/2 order in hydrogen and zero

order in molybdenum hexafluoride with an activation energy of 76000 ± 1500 J/mol. A preexponential factor of $2.02 \times 10^6 \pm 1.21 \times 10^6$ nm s^{-1} $torr^{-0.5}$ was determined. These results were similar to those found in tungsten hexafluoride kinetic studies.

4. Due to the porosity of the molybdenum films and the observed roughness of the Mo-Si interface, molybdenum hexafluoride does not appear to be a good compound for molybdenum LPCVD, under the conditions investigated.

RECOMMENDATIONS

Based on the results of this experimental work and the literature review, the following recommendations are made:

1. Further testing needs to be performed to determine the film purity dependence on temperature and pressure.

2. A transmission electron microscopy (TEM) study would be helpful in analyzing for voids and pores in the films.

3. In order to use AES depth profiling in determining the amount of molybdenum deposited, an oxygen (O^+) ion beam is needed and also the capability of flooding the AES chamber with oxygen. This modification would eliminate the negative effects of oxygen as an impurity.

REFERENCES CITED

REFERENCES CITED

1. Shaw, J.M., and Amick, J.A. RCA Review, p. 306, June, 1970.

2. Sze, S.M., "VLSI Technology", McGraw-Hill: New York, 1983.

3. Ghandi, S.K. "VLSI Fabrication Principles", John Wiley and Sons: New York, 1983.

4. Beidler, E.A.; Powell, C.F.; Cambell, I.E.; and Yntema, L.F. J. Electrochem Soc., 98, 21 (1951).

5. Berezhoni, A.S. "Silicon and its Binary Systems", Transl. from Russ., p. 173, Consultants Bureau, New York (1960).

6. "Refractory Molybdenum Silicides", Bulletin Cdb-6A, p. 9, Climax Molybdenum Co. (May 1963).

7. Simeonov, S.S., Kafedjiiska, E.I., and Guerassimov, A.L. Thin Solid Films, 115, 291-220 (1984).

8. Shroff, A.M., Delval, G. High Temperatures-High Pressures, Vol. 3, p. 695 (1971).

9. Yasuda, K., and Murota, J. Japanese J. of Appl. Phys., Vol. 22, No. 10, p. L615 (1983)

10. Fukumoto, M.; Inoue, K.; Ogawa, S.; Okada, S.; and Kugimiya, K. "1 μm Mo Gate MOS Technology", 1981 Symposium on VLSI Technology, Publ. IEEE, New York

11. Schroff, A.M., Thomson-CSF "Influence of the Pressure on the Deposition Characteristics of CVD Tungsten", 6th Plansee Seminar 1968, Edited by Benesovsky, Springer Verlag, 1969.

12. Seto, D.K., Doo, V.Y., Dash S., "Growth and Characterization of Low Temperature CVD Molybdenum Films", Chem. Vapor Deposition, Int. Conf., 2nd, 659-92, Ed. by: Blocher, J.M., Jr., Electrochem. Soc., New York, (1970).

13. Hieber, K.; Stolz, M.; Siemens, AG Thin Solid Films, 100(3), 209-18 (1983)

14. Casey, J.J.; Verderber, R.R.; and Garnache, R.R. J. Electrochem Soc., Vol. 114, No. 2, 201 (1967).

15. Schroff, A.M. High Temperatures-High Pressures, Vol. 6, 415-421 (1974).

16. Inoue, S.; Toyokura, N.; Nakamura, T.; Maeda, M. and Takugi, M. J. Electrochem. Soc., Vol. 130, No. 7, 1603 (1983).

17. Kaplan, L.H., and d'Heurle, F.M. J. Electrochem. Soc., 117, (5), 693 (1970).

18. McCreary, W.J. Fifth International Conference on Chemical Vapor Deposition, 714, (1975).

19. Carver, G.E., and Seraphin, B.O. Appl. Phys. Lett, 34, (4) (1979).

20. Carver, G.E. Thin Solid Films, (63), 169 (1979).

21. Pinneo, G.G. Proc. of 3rd Int. Cont. on CVD, F.A. Glaski, Ed., American Nuclear Society, Hinsdale, ILL, p. 462 (1972).

22. Ayugawa, M. Paper # 14p-C-14, Fall Meeting of the JAPS, 1984.

23. Guivarc'h, A.; Auvray, P.; Berthou, L.; LeCun, M.; Boulet, J.P.; Henoc, P.; and Pelous, G. J. Appl. Phys., 49, (1) (1978).

24. Sasaki, Y.; Ozawa, O.; and Kameyama, S. IEEE Trans. on Elect. Dev., Vol. ED-27, No. 8 (1980).

25. Lifshitz, N.; Williams, D.S.; Capio, C.D.; and Brown, J.M. "Selective Molybdenum Deposition by LPCVD", AT&T Bell Labs, Murray Hill, New Jersey. To be published.

26. Woodruff, D.W. and Sanchez-Martinez, R.A., In "Tungsten and Other Refractory Metals for VLSI Applications", E.K. Broadbent, Ed., MRS, Pittsburg (1986).

27. JANAF Thermochemical Tables, 2nd Edition, D.R. Stull and H. Prophet, Editors, National Bureau of Standards, Washington, D.C., 1971.

28. McConica, C.M., and Krishnamani, K. "The Kinetics of LPCVD Tungsten Deposition in a Single Wafer Reactor", AICHE Seattle Meeting (1985).

29. Broadbent, E.K. and Ramiller, C.L. J. Electrochem. Soc. Vol. 131, No. 6, 1427 (1984)

30. Chin, J. Nucl. Sci. Abstr. , 23(16), 31326, (1969).

31. Cheung, H. Nucl. Sci. Abstr. , 26(12), 28599, (1972).

32. Blewer, R.S., editor, "Tungsten and Other Refractory Metals for VLSI Applications," E.K. Broadbent, Ed., (Materials Research Society, Pittsburg, PA 1986).

33. Margaritondo, G. and Rowe, J.E., In "Treatise on Analytical Chemistry", Elving, P.J., Bursey, M.M., Kolthoff, I.M., Eds., John Wiley and Sons, New York, 1981, Part I, Vol. 8, Chap 17.

34. Werner, H.W. and Morgan, A.E. In "Treatise on Analytical Chemistry", Elving, P.J., Bursey, M.M., Kolthoff, I.M., Eds., John Wiley and Sons, New York, 1981, Part I, Vol. 10, Chap 5.

35. Cocks, G.G. In "Treatise on Analytical Chemistry", Elving, P.J., Bursey, M.M., Kolthoff, I.M., Eds., John Wiley and Sons, New York, 1981, Part I, Vol. 8, Chap 16.

36. Thornton, P.R. "Scanning Electron Microscopy, Applications to Materials and Device Sciences", Chapman and Hall Ltd., London, 1968, Chap. I.

37. Lee, H.; Swartz, M.L. and Stoffey, D.G. "Scanning Electron Microscopy of Polymers and Coatings", L.H. Princen, Ed., Interscience Publishers, New York, 1971, No. 16, Chap. I.

38. Wells, O.C. "Scanning Electron Microscopy", McGraw-Hill, Inc., New York, 1974, Chap. I.

39. Suito, E., and Uyeda, N. Proc. Jpn. Acad., 32, 117 (1956).

40. Carlson, T.A. "Photoelectron and Auger Spectroscopy", Plenum Press, New York, 1975, Chap. I-V.

41. Fadley, C.S. In "Electron Spectroscopy; Theory, Techniques and Applications", Brundle, C.R. and Baker, A.D., Eds.; Academic Press, New York, 1978; Vol. 2, Chap. I.

42. Fadley, C.S. and Hagstrom, S.B.M. In "X-ray Spectroscopy", Azaroff, L.V., Ed., McGraw-Hill, New York, 1974, Chap. VIII.

43. Riggs, W.M. and Parker, M.J. In "Methods of Surface Analysis"; Czanderna, A.W., Ed.; Elsevier Scientific, New York, 1975, Vol. 1, Chap. IV.

44. "Handbook of Photoelectron Spectroscopy"; Physical Electronics Division, Perkin Elmer Corp., 1979.

45. Chu, W.; Mayer, J.W. and Nicolet, M.A. "Backscattering Spectrometry", Academic Press, Inc., New York, 1978, Chap. I.

46. Sahin, T., Personal Reference, Montana State University Bozeman, Montana, (1987).

47. Farrell, K., Federer, J.J., Schaffhauser, A.C., "Gas bubble formation in metal deposits", in CVD Second International Conference, Los Angeles (Electrochemical Soc., New York, 1970) .

48. Green, M.L.; Ali, Y.S.; Boone; Davidson, B.A.; Feldman, L.C. and Nakahara, S. To be published.

APPENDIX

Sample Calculations

This is the calculation for determining the preexponential factor, k_o.
The kinetic equation for calculating k_o is:

$$k_o = r/(e^{-E/RT} P_{H_2}^{0.5} P_{MoF_6}^{0})$$

where;
r = Reaction rate, (nm/s)
k_o = Pre-exponential factor, (nm/s/torr$^{-0.5}$)
P_{H_2} = Partial pressure of hydrogen, (torr)
P_{MoF_6} = Partial pressure of MoF_6, (torr)
E = Activation energy of the reaction, (J/g-mol)
R = Universal gas constant, (J/g-mol·K)

For this example calculation the following will be used:
r_{ave} = 0.1808 nm/s
P_{H_2} = 0.84 torr
P_{MoF_6} = 0.06 torr
E_a = 76,000 J/mol
R = 8.314 J/g-mol·K
T = 573 K

$$k_o = 0.1808/\{\exp[-76000/(8.314)\cdot(573)]\cdot(0.84)^{0.5}\cdot(0.06)^{0}$$

and;

$$k_o = 1.67 \times 10^6 \text{ nm/s}\cdot\text{torr}^{0.5}$$

MONTANA STATE UNIVERSITY LIBRARIES
3 1762 10024276 5

DATE DUE

HIGH SMITH REORDER #45-230

AMERICAN BINDERIES
2